PHILOSOPHICAL TRANSACTIONS OF THE ROYAL SOCIETY A MATHEMATICAL, PHYSICAL & ENGINEERING SCIENCES

Pattern Formation in Recirculating Flows of Suspensions of Orientable Particles

Andrew J. Szeri

Phil. Trans. R. Soc. Lond. A 1993 **345**, 477-506
doi: 10.1098/rsta.1993.0142

Pattern formation in recirculating flows of suspensions of orientable particles

By Andrew J. Szeri

Department of Mechanical and Aerospace Engineering, University of California, Irvine, California 92717, U.S.A.

Contents

The global, dynamical behaviour of suspensions of small, orientable, non-interacting particles is investigated. Owing to spatial inhomogeneity of the flow field, certain orientations of particles may be favoured in different regions of the flow. Favoured orientations may be deduced from an analysis of the history of flows experienced by a particle along its path. In flows that are time-periodic in the lagrangian frame of the suspended phase (e.g. steady, recirculating flows in the eulerian frame), the orientation dynamics may be characterized by periodic or quasi-periodic attractors. After the decay of initial transients, such attractors lead to the formation of patterns of orientation of the suspended particles that are temporally fixed but spatially varying in the eulerian frame of reference. In effect, these patterns constitute a new type of global ordering of the suspension that arises not from interaction effects among the particles, but rather from the smoothly varying influences of the flow. Examples of these flow-induced patterns are explored in two- and three-dimensional flows that may be produced in the laboratory. The arguments presented are purely kinematical; as such the conclusions regarding pattern formation pertain to steady, recirculating flows whether or not the particles have an effect on the flow field. As the phenomena described herein have not been previously reported as experimental

Phil. Trans. R. Soc. Lond. A (1993) **345**, 477–506
Printed in Great Britain

observations, this work constitutes a theoretical prediction of a new physical phenomenon.

1. Introduction

We consider patterns that arise in the orientation of particles in recirculating flows of suspensions. The particles in question are assumed to be small with respect to length-scales over which the flow varies; thus their orientation evolves in response to the instantaneous local flow field. We neglect brownian effects that may be important for suspensions of extremely small particles. In addition, the particles are supposed to be neutrally buoyant, and to follow the same paths through the flow as fluid particles. Finally, the particles are assumed to be non-interacting; hence the suspensions we consider are dilute.

The patterns that arise are a consequence of dynamical attractors that characterize the evolution of particle orientations with time; these attractors are global in orientation space and along a given recirculating particle path in the flow. The nature of the attractors may be deduced by a geometrical analysis of the orientation evolution equations that properly accounts for the history of local flows seen by a particle on its journey through the flow field.

The patterns are spatially varying orientations or planes of orientations (steady in the eulerian frame) to which all particles are eventually attracted; hence there is a definite, preferred microscopic arrangement of the suspended phase. However, we emphasize that the materials we consider remain liquid. If the suspension were to cease to flow as a liquid, then the patterns would be lost to whatever brownian motion may be present, no matter how small. It is the flowing of the material which itself creates and maintains the patterns.

The initial work on the orientation dynamics of suspended particles concentrated on single particles in steady, homogeneous flow fields. Jeffery (1922) considered ellipsoidal particles in steady, uniform shear flow; Bretherton (1962) studied particles of a more general shape in three-dimensional steady, uniform shear flow. Particles either rotate indefinitely or align in a preferred direction in these simple flow fields. As one might expect, the dynamics of particles are much richer when one considers their response to local flow fields that are time-dependent.

Recent work in this area by Szeri *et al.* (1991) focused on the range of possible dynamical behaviour of orientable particles in two-dimensional flows that are unsteady in the lagrangian frame. Whilst the flows they consider are restricted to two dimensions, however, the particles are free to move out of the plane of the flow. The governing equations for the path and orientation of rigid, neutrally buoyant particles are well-known:

$$\frac{\mathrm{d}}{\mathrm{d}t}\boldsymbol{x}(t) = \boldsymbol{u}(\boldsymbol{x}(t)), \tag{1.1}$$

$$\frac{\mathrm{d}}{\mathrm{d}t}\boldsymbol{R} = \boldsymbol{\kappa}\cdot\boldsymbol{R} - \boldsymbol{\kappa}\colon \boldsymbol{RRR}, \quad \boldsymbol{\kappa} = \boldsymbol{\Omega}(\boldsymbol{x}(t)) + G\boldsymbol{E}(\boldsymbol{x}(t)). \tag{1.2}$$

The orientation of the particles is given by the vector $\boldsymbol{R}(t;\boldsymbol{R}_0)$. The axial vector $\boldsymbol{R}$ rotates in response to the local flow field experienced by the particle, through the dependence of (1.2) on the rate-of-strain tensor $\boldsymbol{E}$, and on the vorticity tensor $\boldsymbol{\Omega}$. The inefficiency of rotation of particles with finite aspect ratio in straining flows is

accounted for by the shape factor G, which normally lies between 0 and 1. Owing to the periodic nature of the particle paths in a *recirculating* flow, note that the equivalent velocity gradient tensor $\boldsymbol{\kappa}$ has periodic dependence on time in that case. It is this source of unsteadiness in the basic equations for particle orientation dynamics that is responsible for the phenomena we shall describe. In the steady, recirculating flows of interest to the present work, particle orientation dynamics is shown by Szeri *et al.* (1991) to be either asymptotically periodic or quasi-periodic. In the first case there is a periodic attractor in the plane of the flow to which all initial orientations are eventually attracted. In the second case, there is no attractor present, and particles simply tumble in an irregular fashion in three dimensions along their respective recirculating paths through the flow field.

These assertions concerning particle orientation dynamics in two-dimensional flow fields were tested in a series of physical experiments reported in Szeri *et al.* (1992), in which observations were made of the orientation dynamics of a rigid particle suspended in a carefully controlled flow in a four-roll mill. In these experiments, a single rigid particle was maintained at a fixed point in the test section of the flow device and subjected to a well-characterized, time-periodic local flow. The experiment as described was intended to simulate the flow-induced dynamics of a particle that experiences a time-periodic variation in the local flow as it circumnavigates a recirculating path through a spatially inhomogeneous flow that is steady in the eulerian frame of reference. Quasi-periodic dynamics and dynamics associated with the presence of a periodic attractor were observed for different periodic protocols of the local flow field, in accord with theoretical predictions.

More recently, the analytical tools for the study of particle orientation dynamics were extended to the case of particles suspended in three-dimensional flows in Szeri & Leal (1993). There, it is shown that the only *generic* types of dynamical behaviour of particles suspended in recirculating, three-dimensional flow fields are dynamics associated with a periodic attractor, or with a quasi-periodic attractor. These results seem, at first glance, to be at odds with the results for particle orientation dynamics in two-dimensional flow fields, in which there is no attractor associated with the quasi-periodic dynamics. The resolution of this paradox is rather subtle. Upon close examination, it is clear that the structurally unstable quasi-periodic orientation dynamics that may arise in a two-dimensional flow perturbs to dynamics associated with a structurally stable quasi-periodic attractor in a nearby, slightly three-dimensional flow. For a thorough discussion of the relevant issues of structural stability of dynamical systems, we refer the reader to Arnold (1988). Notwithstanding these subtle differences of particle orientation dynamics in two- and three-dimensional flows, the two generic possibilities for recirculating flows are as follows. Either the orientation dynamics is asymptotically periodic, or the orientation dynamics is asymptotically quasi-periodic.

The three papers just described have in common a local point of view, that is to say that each is focused on the details of the particle orientation dynamics of a single particle that follows a specific recirculating path through the flow. The task of this work is to synthesize the information regarding particle orientation dynamics of single particles into a coherent picture of what will happen in the entire flow field. To construct this coherent picture of the flow field, it will be important to consider what may be the relation between attractors for the particle orientation dynamics associated with neighbouring particle paths. When we have established that the variation in such attractors across particle paths must be smooth, it is clear that

PHILOSOPHICAL TRANSACTIONS OF THE ROYAL SOCIETY A MATHEMATICAL, PHYSICAL & ENGINEERING SCIENCES

there must be regions of the flow domain in which smoothly varying patterns characterize the distribution of particle orientations after the decay of initial transients. However, owing to the various types of attractors for the particle orientation dynamics (periodic and quasi-periodic), and as a consequence of the topology of the phase space of the differential equation for orientation of particles, some unexpected and subtle patterns arise in recirculating flows of suspensions. The patterns we describe should be observable via optical techniques (see, for example, Frattini & Fuller 1986) with suitable materials. A more direct way to observe the patterns would be to solidify a flowing matrix in which the pattern is generated by a Stokes flow; we discuss this possibility below.

We begin our analysis with steady, recirculating two-dimensional flows in §2, in which case it proves to be convenient to work in terms of the stream function. After some initial background discussion on particle orientation dynamics in such flows, we find that a periodic attractor for the orientation dynamics, where it exists, must vary smoothly across level sets of the stream function. This is reflected by the smoothly varying patterned zones one observes in examples. In addition, there may be thin bands of quasi-periodic particle dynamics that separate patterned zones characterized by different particle orientation dynamics. The patterned zones separated by such a thin band of quasi-periodic dynamics may differ in a fundamental way: namely, the particles in the different patterned zones may differ in the number of end-over-end flips that each particle undergoes around a circuit. These differences between distinct patterned zones in the flow reflect topological restrictions on the phase space of the differential equation for orientation dynamics. The patterned zones, together with thin bands of quasi-periodic behaviour, are investigated in detail for an example flow that occurs between eccentric, co-rotating cylinders.

In §3, we alter the focus to three-dimensional flow fields. As our concern is with particles that follow recirculating paths through the flow field, we first examine the geometric nature of recirculating flows in three dimensions. This leads to some consideration of the hamiltonian structure of the particle paths in these flows. With some knowledge of the particle paths, it is then possible to investigate the variation of attractors for the particle orientation dynamics across particle paths. In three dimensional flows, where there may be quasi-periodic as well as periodic attractors, we find that quasi-periodic attractors in the lagrangian frame correspond to fixed attracting invariant planes in orientation space in the eulerian reference frame. Hence, in recirculating flows in three dimensions, there are in fact two globally ordered states of the flowing suspension. One state is characterized by a dominant single orientation of particles at each point of space. The second state is characterized by a dominant plane of orientations of particles at each point of space. The two states of the flowing suspension may coexist side-by-side in a single flow field. These phenomena are investigated in detail in an example flow within a viscous, spherical drop suspended in a linear external flow field, after Stone *et al.* (1991).

Finally, in §4, we give our conclusions. In addition, we include some speculation on the uses to which these phenomena may be put.

2. Pattern formation in steady, recirculating, two-dimensional flows

In this section, we first review what is known about the orientation dynamics of particles in two-dimensional flow field. Next, as an initial step towards constructing a coherent picture of particle orientation dynamics in regions of the flow, we study

PHILOSOPHICAL TRANSACTIONS OF THE ROYAL SOCIETY A MATHEMATICAL, PHYSICAL & ENGINEERING SCIENCES

the orientation dynamics of particles that follow neighbouring particle paths. This leads to the description of the structure of patterned zones in the flow field, that are finally investigated in detail for an example flow.

(*a*) *A brief discussion of particle orientation dynamics in two-dimensional flows*

Now we turn our attention to the analysis of particle orientation dynamics in two-dimensional flows. In a two-dimensional flow field, in which the flow occurs in the x–y plane, and the vorticity vector is parallel to the z-axis, equation (1.1) takes the special form:

$$\mathrm{d}x/\mathrm{d}t = u(x(t), y(t)), \tag{2.1a}$$

$$\mathrm{d}y/\mathrm{d}t = v(x(t), y(t)), \tag{2.1b}$$

where u and v are the components of the velocity field in the x and y directions respectively. For the following discussion, we assume that the velocity field (u, v) is known in terms of a steady stream function $\psi(x, y)$, with compact level sets. We assume further that the particle paths $(x(t;\psi), y(t;\psi))$ are recirculating; thus $x(t;\psi) = x(t+T_\psi;\psi)$, $y(t;\psi) = y(t+T_\psi;\psi)$, where T_ψ is the period.

It is profitable to describe the space of orientations of the particles relative to modified spherical polar coordinates (σ, θ), defined as follows. The angle σ is measured from the positive x-axis in the x–y plane in the usual, positive sense. The angle θ is $\frac{1}{2}\pi$-Θ, where Θ is the usual angle measured from the positive z-axis in standard definitions of spherical polar coordinates. With these definitions, when a particle lies in the plane of the flow, $\theta = 0$. Equation (1.2) may be written in these coordinates in the form

$$\mathrm{d}\sigma/\mathrm{d}t = \tfrac{1}{2}\omega - Ge\sin 2\sigma + \tfrac{1}{2}G\gamma\cos 2\sigma, \tag{2.2a}$$

$$\mathrm{d}\theta/\mathrm{d}t = -\tfrac{1}{2}G(e\cos 2\sigma + \tfrac{1}{2}\gamma\sin 2\sigma)\sin 2\theta. \tag{2.2b}$$

The flow parameters e, γ and ω are components of the rate-of-strain and vorticity tensors evaluated at the current position of the particle:

$$\boldsymbol{E} = \begin{bmatrix} e & \frac{1}{2}\gamma & 0 \\ \frac{1}{2}\gamma & -e & 0 \\ 0 & 0 & 0 \end{bmatrix}, \quad \boldsymbol{\Omega} = \begin{bmatrix} 0 & -\frac{1}{2}\omega & 0 \\ \frac{1}{2}\omega & 0 & 0 \\ 0 & 0 & 0 \end{bmatrix}.$$

The parameters e, γ and ω depend on time owing to the motion of the particle through the spatially inhomogeneous velocity field. Thus, the differential equations (2.2) experience time-periodic forcing.

In equations (2.2*a*, *b*) the role played by the shape factor G may be understood as follows. Spherical particles ($G = 0$) simply rotate with the local vorticity. Fibres of infinite aspect ratio ($G = 1$) rotate and align exactly as a line element of the fluid. Moderate aspect ratio particles respond anisotropically in a way that depends on G; one observes that G multiplies the anisotropic contribution to the vector field corresponding to the right-hand-side of equations (2.2*a*, *b*). Hence, attractors for the orientation dynamics are more likely to occur if G is closer to 1.

If we were to conduct an investigation into the vector form of the orientation evolution equation (1.2) for particles in a steady, recirculating, two-dimensional flow field, it would be convenient to proceed in the following manner. Rather than considering individual time-traces of equation (1.2), it is more profitable when

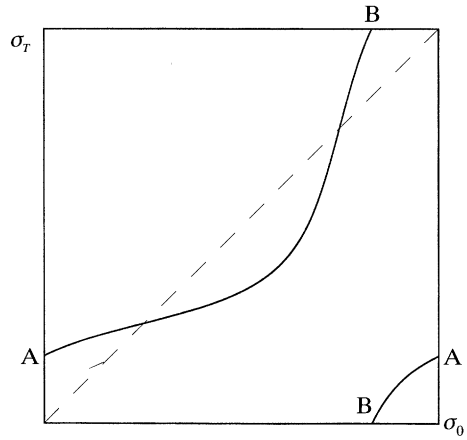

Figure 1. Form of the Poincaré map $\mathscr{P}_\psi$ of the in-plane orientation angle of a particle on a recirculating path in a two-dimensional flow. The points (A, A) and (B, B) are equivalent. The Poincaré map must be one-to-one, onto, and differentiable with differentiable inverse (a diffeomorphism). A transverse intersection of $\mathscr{P}_\psi$ with the dashed line $\sigma_T = \sigma_0$ corresponds to a periodic integral curve. If the slope of $\mathscr{P}_\psi$ at the point of insection is less than one, the corresponding periodic integral curve is an attractor.

investigating a periodically forced system of equations to work in terms of the Poincaré map, defined by

$$\mathscr{P}_\psi(\boldsymbol{R}_0) = \boldsymbol{R}(T_\psi;\, \boldsymbol{R}_0,\, \psi). \tag{2.3}$$

In equation (2.3), $\boldsymbol{R}(t;\, \boldsymbol{R}_0,\, \psi)$ is the solution of equation (1.2) with initial condition $\boldsymbol{R}_0$ for a particle that follows the particle path on the level set of the stream function ψ. One application of the Poincaré map is equivalent to integrating equation (1.2) forward over one period of the flow. Of course, the period of the flow, the precise nature of the forcing of equation (1.2), and hence the Poincaré map all depend on the level set of the stream function ψ on which the particle-path resides. The graph of the Poincaré map, $\{\boldsymbol{R}_0,\, \mathscr{P}_\psi(\boldsymbol{R}_0)\}$, is constructed from the solutions of (1.2) over one period of the flow, over the range of possible initial orientations $\boldsymbol{R}_0$.

In the special case of two-dimensional flow fields that we now consider, it is apparent upon examination of the system (2.2) that the orientation dynamics of particles in the σ and θ coordinates is decoupled. It happens that the dynamics in θ are determined by the dynamics in σ, and that the dynamics in σ are decoupled from the dynamics in θ. Hence it is sufficient to consider the reduced Poincaré map

$$\mathscr{P}_\psi(\sigma_0) = \sigma(T_\psi;\, \sigma_0,\, \psi) \tag{2.4}$$

in the study of particle dynamics in two-dimensional flow fields.

Owing to the fact that the reduced Poincaré map is defined from the flow of the differential equation (2.2a) evaluated over the period T_ψ, it must be one-to-one, onto and differentiable with differentiable inverse (i.e. a diffeomorphism). Hence, for the case where there is an attractor for the orientation dynamics, it must appear as shown in figure 1; the interested reader may consult Szeri *et al.* (1991) for details of this argument. Figure 1 is drawn with both the domain and range modulo π, as $0 \leqslant \sigma < \pi$ is the range of the variable σ (owing to fore-and-aft symmetry of the particle).

As shown in figure 1, an intersection of the Poincaré map with the line $\sigma_T = \sigma_0$ corresponds to a periodic solution of the underlying differential equation, owing to the definition of $\mathscr{P}_\psi(\sigma_0)$. When $\mathrm{d}\mathscr{P}_\psi/\mathrm{d}\sigma_0 < 1$ at a point of intersection $\sigma_0 = \mathscr{P}_\psi(\sigma_0)$, the

associated periodic solution is a T_ψ periodic attractor. For particles for which there is no intersection of $\mathscr{P}_\psi(\sigma_0)$ with $\sigma_T = \sigma_0$, the dynamics are quasi-periodic. It is possible that when there is no intersection of the Poincaré map with the line $\sigma_T = \sigma_0$, there may be a periodic attractor of period kT_ψ, $k > 1$. However, the result will not be a steady pattern in the eulerian reference frame, and so we do not distinguish this case from that of truly quasi-periodic motion.

When viewed in a fixed eulerian frame of reference, these considerations have the following interpretation. A T_ψ periodic solution of the orientation evolution equation superposed on a T_ψ periodic solution to the particle path equations corresponds to a *steady* orientation at all points along the particle path when viewed in a fixed eulerian frame of reference. If the T_ψ periodic solution is an attractor, then other initial orientations within the basin of attraction (in orientation space) will eventually settle down to a steady orientation in the eulerian frame. We remark that Szeri *et al.* (1991) show that an attractor for the orientation dynamics in two-dimensional flow is an integral curve of the orientation evolution equation that must lie in the plane of the flow. A quasi-periodic solution of the orientation evolution equation superposed on a T_ψ periodic solution to the particle path equations corresponds to an *unsteady* orientation at all points along the particle path when viewed in a fixed eulerian frame of reference. Thus, as mentioned before, the particle tumbles in three dimensions.

Now, two neighbouring particle paths, $(x(t;\ \psi),\ y(t;\ \psi))$ and $(x(t;\ \psi+\delta\psi),\ y(t;\ \psi+\delta\psi))$ have differing initial conditions. The solutions to the system (2.1) and (2.2) depend smoothly on the initial condition. Furthermore, solutions may be extended backwards and forwards indefinitely in time, owing to the fact that the phase space is a compact manifold (the compact level sets of the stream function). Thus the Poincaré map must also vary smoothly with stream function, for those level sets on which it is defined. Note that the Poincaré map is not defined, for example, on the level set of the stream function which happens to be the stable manifold of a saddle point in the flow field. The reason for this is that the associated particle path is not periodic.

We have established that the Poincaré map must vary smoothly with ψ. Hence, when there is a *transverse* intersection of $\mathscr{P}_\psi(\sigma_0)$ with $\sigma_T = \sigma_0$ for a given recirculating path-line ψ, then a neighbouring path-line $\psi+\delta\psi$ will also show a transverse intersection of $\mathscr{P}_{\psi+\delta\psi}(\sigma_0)$ with $\sigma_T = \sigma_0$; see figure 2. Thus, attractors deform smoothly from one nested stream-line to another. This leads to the existence of attractors for the orientation dynamics of particles that extend over a region of the flow.

(*b*) *Conditions that apply near an elliptic stagnation point*

As a simple but useful illustration of these concepts, we consider the dynamics of particles that follow the recirculating path-lines in the neighbourhood of an elliptic stagnation point in the flow field. We fix cartesian coordinates $(\xi,\ \eta)$ so the elliptic point is at the origin, and the flow occurs in the ξ–η plane. The stream function in the neighbourhood of the origin may be written

$$\psi(\xi,\eta) = \tfrac{1}{2}\{\xi\ \eta\}\begin{bmatrix}\psi_{,\xi\xi} & \psi_{,\xi\eta}\\ \psi_{,\xi\eta} & \psi_{,\eta\eta}\end{bmatrix}\begin{Bmatrix}\xi\\ \eta\end{Bmatrix}+\ldots.$$

The derivatives are evaluated at the origin. For simplicity, we write $a = \psi_{,\xi\xi}$, $b = \psi_{,\xi\eta}$ and $c = \psi_{,\eta\eta}$, with $b^2 - ac < 0$ for elliptic stream lines.

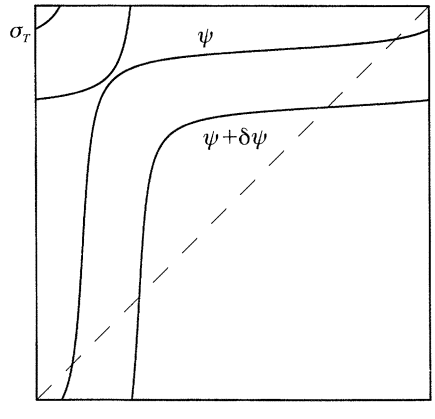

Figure 2. Change in $\mathscr{P}_\psi$ for a small change in ψ. Note that a transverse intersection of $\mathscr{P}_\psi(\sigma_0)$ with the dashed line $\sigma_T = \sigma_0$ is preserved for small changes in ψ, hence, attractors for the orientation dynamics deform smoothly across particle paths.

For particles that follow the level sets of ψ near the origin, the velocity gradient evaluated along the particle path is steady to leading order. In other words, to leading order, the velocity gradient tensor evaluated on particle paths near the origin is simply the velocity gradient at the origin. Hence the particle dynamical equation (2.2) is autonomous. Szeri *et al.* (1991) show that particles in a flow that is locally steady in the lagrangian frame will rotate if the discriminant D is negative; for this flow, one may compute

$$D = 4G^2b^2 - 2(1+G^2)\,ac + (G^2-1)\,(a^2+b^2).$$

D is negative for $G \leqslant 1$, owing to the inequality $b^2 - ac < 0$. The period of end-over-end rotation (by π) appears in the Appendix of Szeri *et al.* (1992):

$$T_{\text{flip}} = 2\pi/\sqrt{(-D)}.$$

The period of the particle path, in contrast, is

$$T_{\text{path}} = 2\pi/\sqrt{(ac-b^2)}.$$

This latter result is easily established by integrating the particle-path equations near the elliptic stagnation point. It is interesting to note that when $G = 1$, $T_{\text{path}} = 2T_{\text{flip}}$; thus, particles of infinite aspect ratio perform exactly two end-over-end flips during each circumnavigation of the elliptic point. Particles of finite aspect ratio ($G < 1$) have incommensurate periods of rotation and circumnavigation, in general. Even when the periods of rotation and circumnavigation happen to be commensurate, however, there is no attractor for the orientation dynamics. This proves the assertion that every elliptic stagnation point in a two-dimensional flow of a suspension will be surrounded by a non-patterned (i.e. quasi-periodic) zone.

(*c*) *Structure of patterned zones*

In this sub-section, we investigate the structure of patterned zones. The first question to answer is, what might constitute the boundary of a patterned zone? Clearly, it may happen that at some particular level set of the stream function ψ^*, the Poincaré map $\mathscr{P}_{\psi^*}(\sigma_0)$ has a degenerate intersection with the curve $\sigma_T = \sigma_0$, i.e. an intersection at which $\mathrm{d}\mathscr{P}_\psi/\mathrm{d}\sigma_0 = 1$, as shown in figure 3.

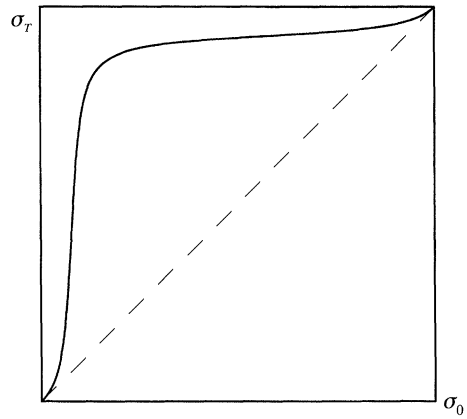

Figure 3. $\mathscr{P}_\psi$ at a critical set of ψ, where a saddle-node bifurcation occurs. This map is actually taken from the example in §2*d*, on the particle path anchored at $(x, y) = (2.068, 0)$.

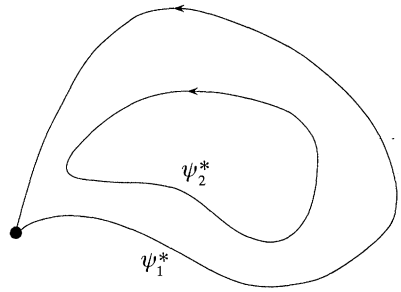

Figure 4. Sketch of a region bounded by two critical level sets of ψ, within which there is a periodic attractor for the orientation dynamics of particles associated with each particle path.

This is the point of saddle-node bifurcation of the Poincaré map, at which the associated periodic integral curve is neither an attractor nor a repellor but rather a degenerate, meta-stable object. On one side of ψ^*, there will be a periodic attractor and on the other side of ψ^* the dynamics will be quasi-periodic. For this reason, the level set ψ^* is a boundary between a region of steady pattern (in an eulerian reference frame) and one of no pattern. Another type of boundary is one where the level set ψ contains a stagnation point. We shall refer to either possibility as a *critical* level set of ψ.

Now that we have established what constitutes the boundary of a patterned zone, let us consider the nature of attractors for the orientation dynamics of particles with particle paths that lie between two critical level sets, say, ψ_1^* and ψ_2^*, as shown in the sketch in figure 4.

One interesting fact that relates all the attractors in the patterned zone $\psi_1^* < \psi < \psi_2^*$ is that the particles on all the level sets of ψ flip the same number of times. To see this, consider the number of end-over-end flips characterizing a given attractor,

$$n(\psi) = \frac{1}{\pi}[\sigma_\psi^*(T_\psi;\, \sigma_0^*) - \sigma_\psi^*(0;\, \sigma_0^*)]. \tag{2.5}$$

In (2.5), σ_ψ^* is an attractor for the orientation of particles on a given level set ψ. Note that in equation (2.5), σ^* is to be computed in the extended coordinate system in which σ is not taken modulo π. The number of end-over-end flips n is the (integer)

number of net rotations of the particle by π as it moves around the particle path. Now, consider two neighbouring, nested streamlines ψ and $\psi+\delta\psi$ in the patterned zone between the two critical level sets ψ_1^* and ψ_2^*. The attractor must be a smoothly changing object with ψ, hence

$$n(\psi+\delta\psi) = \frac{1}{\pi}[\sigma^*_{\psi+\delta\psi}(T_{\psi+\delta\psi}) - \sigma^*_{\psi+\delta\psi}(0)]$$

$$= \frac{1}{\pi}[\sigma^*_{\psi}(T_{\psi}) - \sigma^*_{\psi}(0) + O(|\delta\psi|)] = n(\psi).$$

The last step in this calculation makes use of the fact that $n(\psi)$ must be an integer. This simple argument may be continued by induction to all the particle paths in the patterned zone $\psi_1^* < \psi < \psi_2^*$.

These arguments have the following logical extension: patterned zones that are characterized by a different flip number must be separated by either a quasi-periodic zone, or by a critical level set of ψ. Topologically, this statement is easily understood. The appropriate phase space in which the evolution equation for σ should be analysed is a torus, with coordinate σ around one circular generator and periodic time τ around the other. A periodic attractor is a closed curve that lies on the surface of the torus, and passes through the 'hole' a net $n(\psi)$ times in a period. An attractor with n flips cannot smoothly transform into an attractor with $m \neq n$ flips as these two objects are of fundamentally different topological type. In topological terms, the two attractors belong to different homotopy classes. We return to these deliberations in more detail in §3*d*.

Finally, we remind the reader that when the flow is strictly two-dimensional, the quasi-periodic dynamics are not associated with an attractor, strictly speaking. However, as we discuss in §3, under a slight three-dimensional perturbation to the flow field, the quasi-periodic dynamics in a strictly two-dimensional flow perturbs to dynamics associated with a quasi-periodic attractor. Therefore, although it is not quite accurate, we shall always write in terms of periodic and quasi-periodic attractors, even in strictly two-dimensional flows.

(*d*) *Example: particles in the flow between eccentric rotating cylinders*

Now we shall move on to consider a specific, realistic example flow of a suspension to observe just how the global structures we have discussed may arise. The example flow we analyse occurs between eccentric, co-rotating cylinders. It is a useful flow that may contain such features as free hyperbolic stagnation points and multiple recirculation zones, depending on the choices of various parameters. We refer the reader to the work of Ballal & Rivlin (1977) for a thorough discussion of this flow.

Although the arguments we have presented regarding pattern formation in recirculating flows are purely kinematical, and as such are independent of whether or not the particles have an effect on the flow field, it is simpler in an example flow if we assume that the particles have no effect on the flow field. We remark that this is a reasonable approximation in the limit of infinite dilution of the suspension. Moreover, we consider the Stokes flow between the cylinders under the assumption that the Reynolds number based on the length scale of the flow is small. Note, however, that our previous arguments regarding pattern formation do not require that the flow Reynolds number be small, but only that the particle Reynolds number be small.

PHILOSOPHICAL TRANSACTIONS OF THE ROYAL SOCIETY A MATHEMATICAL, PHYSICAL & ENGINEERING SCIENCES

With these comments out of the way, we proceed with the example. The two cylinders have radii 0.3 and 1, and are arranged with eccentricity 0.75. The inner cylinder rotates anti-clockwise at a non-dimensional angular speed of 20; the outer cylinder rotates with an angular speed of 1. This rather extreme choice of geometric and rotation rate parameters leads to an interesting situation of free hyperbolic and elliptic stagnation points in the (Stokes) flow, with four separate recirculation cells. For the purposes of discussion, we refer to the recirculation cells as A, within the outer cylinder; B, surrounding the inner cylinder; and C and D, to the right of the inner cylinder, left to right. These four cells may be observed in figure 5, below, or in fig. 14*e* of Ballal & Rivlin (1977).

Owing to the complexity of the velocity field, we must integrate the particle-path equations (2.1) and the orientation evolution equation (2.2*a*) numerically, using standard methods. For the shape factor, we take the fairly typical value $G = 0.9$, which corresponds to a fiber-like particle of finite aspect ratio. The Poincaré map associated with each particle path is constructed by integration of (2.2*a*) over the range of initial orientations and over the period of the associated particle path. Upon examination, each such Poincaré map reveals whether the particle dynamics on a given path are characterized by a periodic attractor, or are quasi-periodic. When there is a periodic attractor, the periodic solution of (2.2*a*) this is easily computed by numerical integration, beginning at the initial orientation obtained from the intersection of Poincaré map with the line $\sigma_T = \sigma_0$, which is obtained numerically.

This procedure has been carried out for the entire flow domain in the problem. The result is shown in figure 5, and in detail in figure 6*a–d*, below. In figure 5, information about the particle dynamics is conveyed according to the following scheme. Where there is a patterned zone of particle orientations, this is indicated by a sequence of directors showing the instantaneous orientation of the attractor at various points along the associated recirculating particle path. These orientations are fixed relative to an eulerian frame of reference. Where the behaviour is quasi-periodic, this is indicated by a light grey shade. The solid cylinders appear as dark grey.

The dominant features one observes in figure 5 are the large quasi-periodic (grey) zones: surrounding the inner cylinder (cell B), just within the outer cylinder (cell A), and surrounding the elliptic stagnation points in cells C and D. The quasi-periodic zones surrounding the elliptic stagnation points are in accord with the arguments presented previously. In addition, one may observe two rather thin quasi-periodic bands between patterned zones, one each within cells A and C. These thin quasi-periodic bands serve to separate patterned zones where the attractors have different flip numbers. We shall return to this point later.

Another point of interest in figure 5 is the loss of symmetry. The streamlines of the *flow* are symmetric with respect to the transformation $y \to -y$. However, the attractors, where they are present, deviate strongly from this symmetry. As an example, note the differences in the inner patterned zone in cell C. Directors in the upper half plane tend to point toward the saddle point on the boundary of cell C, but directors in the lower half plane tend to point in a direction parallel to the path-lines. The source of this loss of symmetry is, of course, the directional nature of the particle paths through the flow field.

Now we turn our attention to the patterned zones in the flow. In general, one observes smooth changes of the directors as one jumps across path-lines in the patterned zones, in accord with the theoretical arguments presented earlier. This is readily seen in figure 6*a*, a detailed picture of cell A. In particular, note that the areas

PHILOSOPHICAL TRANSACTIONS OF THE ROYAL SOCIETY A MATHEMATICAL, PHYSICAL & ENGINEERING SCIENCES

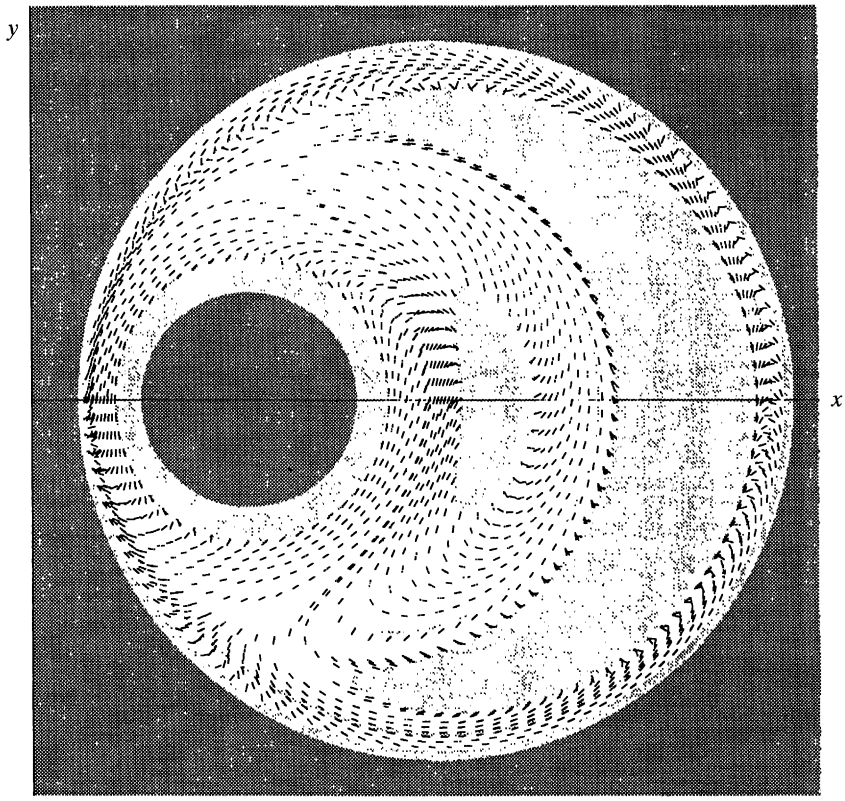

Figure 5. Overview of the example in §2, in which particles ($G = 0.9$) are suspended in the steady flow between eccentric, co-rotating cylinders (dark grey). The counter-clockwise speeds of rotation of the cylinders are (inner) 20 and (outer) 1. The directors indicate the attractors in patterned zones; light grey zones are characterized by quasi-periodic dynamics. The four recirculating regions are denoted A (just within the outer cylinder), B (around the inner cylinder), and C and D, to the right of the inner cylinder, left to right.

where particles rotate more quickly than the path lines turn are shared across path-lines within a given patterned zone. In this way, all the path-lines in a given patterned zone are characterized by the same number of flips.

Of particular interest in figure 6*a* is the thin, quasi-periodic band that separates the two patterned zones of cell A. The outer patterned zone is characterized by +3 flips as particles circumnavigate their recirculating paths. The inner patterned zone shows an additional flip in the upper left-hand portion of figure 6*a*; thus the inner patterned zone is characterized by +4 flips. These two patterned zones with a different number of flips are separated by a thin band of quasi-periodic particle dynamics, as expected. This is in accord with our theoretical predictions. Locally, the extra flip in the inner patterned zone is observed to arise smoothly. However, the inner and outer patterned zones cannot fit together globally, and so a thin quasi-periodic band forms to enable the transition.

Cell B, shown in an expanded view in figure 6*b*, has but one patterned zone and one quasi-periodic zone. The patterned zone is characterized by 0 net flips around each circuit.

In cell C, we again have four zones of particle behaviour. This can be seen in detail in figure 6*c*. Proceeding from the outside inward, the zones are patterned with −1

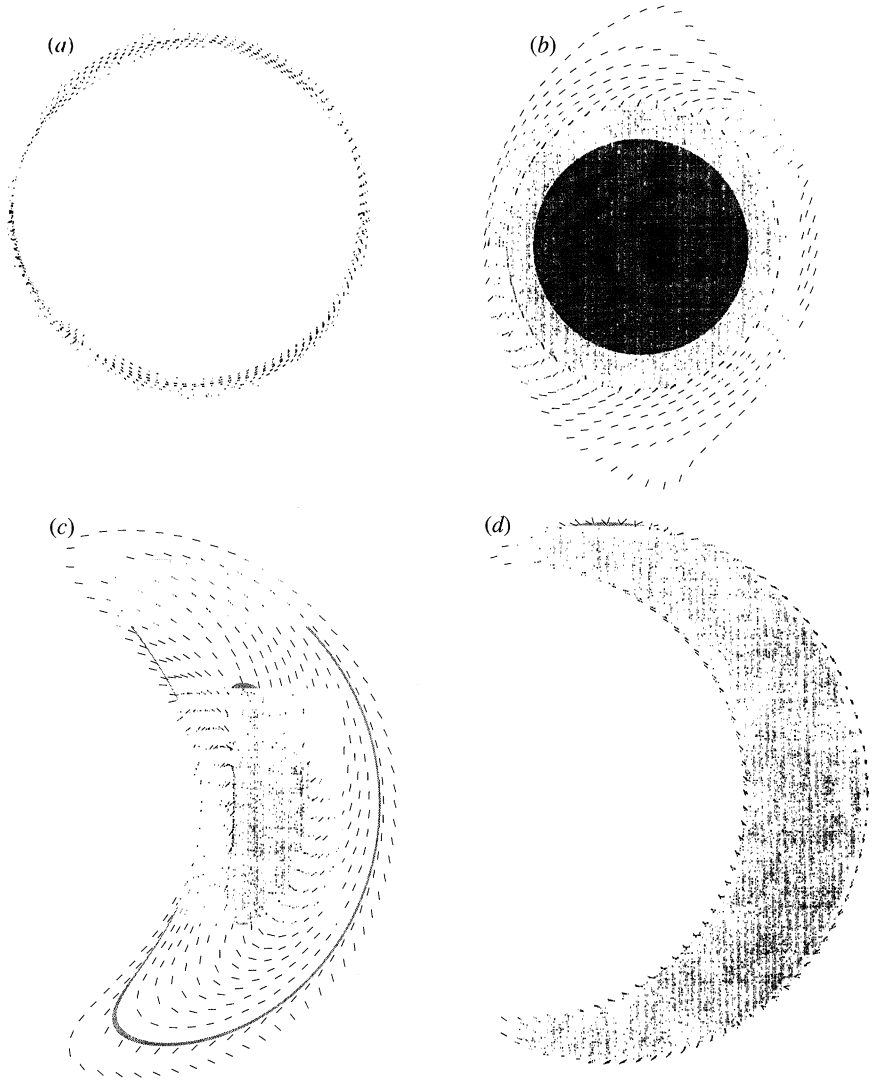

Figure 6. (*a*) Detail of the four nested zones in cell A. Proceeding from the outside inward, the zones are quasi-periodic, patterned (+3 flips), quasi-periodic, and patterned (+4 flips). (*b*) Detail of the two nested zones in cell B. Proceeding from the outside inward, the zones are patterned (0 flips), and quasi-periodic. The dark circle is the inner cylinder. (*c*) Detail of the four nested zones in cell *C*. Proceeding from the outside inward, the zones are patterned (−1 flips), quasi-periodic, patterned (−2 flips), and quasi-periodic. (*d*) Detail of the two nested zones in cell D. Proceeding from the outside inward, the zones are patterned (+3 flips), and quasi-periodic.

flip, then there is a thin quasi-periodic band, then a patterned zone of −2 flips, and finally a quasi-periodic zone that contains the elliptic stagnation point as an interior point. The additional (positive) rotation in the attractors in the outer patterned zone in cell C occurs near the lower extremity of cell C. Again, we observe a thin band of quasi-periodic particle dynamics separating two patterned zones of distinct flip number. Finally, cell D in figure 6*d* shows a very large inner zone of quasi-periodic behaviour. This area is surrounded by a patterned zone of +3 flips.

In figure 7, we explore the structure of the quasi-periodic band in cell C in detail,

PHILOSOPHICAL TRANSACTIONS OF THE ROYAL SOCIETY A MATHEMATICAL, PHYSICAL & ENGINEERING SCIENCES

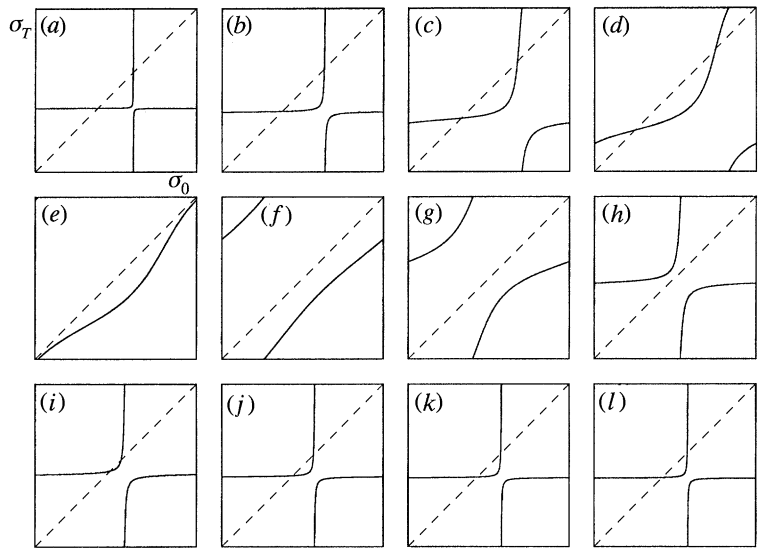

Figure 7. Poincaré maps computed at different level sets of the stream function proceeding within cell C through the three outer zones: patterned (−1 flips) (*a*)–(*d*), the thin quasi-periodic band (*e*)–(*h*), patterned (−2 flips) (i)–(l). The particle paths of (*a*)–(*l*) are anchored at $y = 0$ and $x = 1.106$, 1.108, 1.109, 1.1094, 1.1096, 1.1098, 1.11, 1.111, 1.112, 1.114, 1.116, 1.118, respectively.

by an examination of the Poincaré maps associated with successively nested particle paths that span the thin quasi-periodic band. Specifically, figure 7 includes 12 Poincaré maps, computed for nested pathlines that lie in the outer, patterned zone (−1 flips) through the quasi-periodic band and into the inner patterned zone (−2 flips). One can see that the Poincaré map changes rapidly, albeit continuously, from nested path-line to path-line, i.e. from figure to figure. In figure 7*a–d*, one clearly observes a single stable fixed point of the Poincaré map corresponding to the attractor for orientation dynamics for particles in the outer patterned zone. On a path-line between those associated with figure 7*d*, *e* the fixed point of the Poincaré map is annihilated in a saddle-node bifurcation. This occurs on a critical level set of ψ. In figure 7*e–h*, there is no fixed point of the Poincaré map; hence the behaviour is quasi-periodic. Physically, this corresponds to a non-patterned zone in the eulerian frame of reference; the non-patterned zone is indicated by the thin grey band in figure 6*c*. Finally, the attractor re-emerges after another saddle-node bifurcation of the Poincaré map, which occurs on a path-line between those associated with the Poincaré maps of figure 7*h*, *i* (another critical level set of ψ). The fixed point is again visible in figure 7*i–l*, where the associated path-lines lies in the inner patterned zone of cell C.

It is interesting to observe that the attractor in the outer patterned zone of cell C seems to have developed one additional (positive) flip relative to the attractor in the inner patterned zone, in order that there may be a smooth transition between the attractor in the outer path-lines of cell C and those of cell D. Note that the extra positive flip of particles on the outer right side of cell C (figure 6*c*) matches the positive flip of particles on the outer left side of cell D (figure 6*d*).

In view of the dependence of the particle dynamics on the shape factor G, one would expect the patterns we have described to change if G were different from 0.9.

As we have indicated, G controls the anisotropic contribution to the particle orientation dynamics. Hence G near 1 is associated with a greater likelihood of an attractor. If G were increased from 0.9, one would expect that patterned zones would develop over a greater portion of the flow field.

In summary, in this example flow of a suspension, the principal features of pattern formation that we have described in detail were observed in a numerical example flow. These features include: (i) smoothly varying patterned zones where there was a periodic attractor for the orientation dynamics, (ii) a like number of end-over-end flips of all attractors in the same patterned zone, (iii) zones of quasi-periodic dynamics surrounding elliptic stagnation points, and (iv) thin bands of quasi-periodic dynamics separating patterned zones with distinct flip numbers.

3. Pattern formation in steady, recirculating, three-dimensional flows

In this section, we change the focus of our study to three-dimensional flows of suspensions. First, we consider particle paths in recirculating three-dimensional flows. Next, we review the orientation dynamics of particles suspended in three-dimensional flows. This leads to an analysis of pattern formation in the neighbourhood of elliptic stagnation points. Next, the structure of the various types of patterned zones is then explored in detail. Finally, we consider an example of a fully three-dimensional flow in which these phenomena may be observed.

Pattern formation in three-dimensional recirculating flows is considerably more complex than in two-dimensional flows for three principal reasons. The first reason is that the geometry of particle paths is more complex in three dimensions; they lie not simply on levels sets of the stream function, but rather on level sets of two globally defined functions of the three spatial coordinates. In addition, the concept of nested particle paths does not apply in three-dimensional flows.

The second principal reason for the differences of three-dimensional versus two-dimensional flows of suspensions has to do with the attractors for the orientation dynamics. In three-dimensional flows, a quasi-periodic attractor for the orientation dynamics superposed on the associated periodic particle path leads to a rich patterned structure that is fundamentally different from the patterned structure associated with periodic attractors. Whereas the eulerian picture of a periodic attractor for the orientation dynamics is characterized by an attracting single, steady orientation along the particle path, the eulerian picture of a quasi-periodic attractor is characterized by an *attracting plane* of particle orientations at each point along the path. In two-dimensional flows, recall, there was no fixed pattern associated with quasi-periodic dynamics.

Finally, the third principal difference between two and three dimensional flows of suspensions concerns the variation of attractors for the orientation dynamics across particle paths. In two dimensional flows, we deduced that attractors for the orientation dynamics may belong to different homotopy classes, which has the physical interpretation of differing numbers of end-over-end flips per circuit around the recirculating path. In three-dimensional flows, the topological nature of the phase space for the orientation dynamics problem changes, with the effect that a bridge between the different homotopy classes is formed. Hence, in three-dimensional flows of suspensions, there is no phenomenon analogous to the thin quasi-periodic bands that must separate patterned zones with different flip numbers. Instead, there are simply two states of the flowing suspension that may co-exist side by side after

PHILOSOPHICAL TRANSACTIONS OF THE ROYAL SOCIETY A MATHEMATICAL, PHYSICAL & ENGINEERING SCIENCES

the decay of initial transients: these are characterized by a steady field of predominant orientations or by a steady field of predominant planes of orientations of the suspended particles. We consider these new complications in turn, and then move on to consider an example flow with three-dimensional recirculating particle paths.

(a) *Topological considerations and hamiltonian structure of particle paths*

In a two-dimensional steady flow, path-lines correspond to level sets of the stream function, a constant of the motion that may be profitably regarded as the hamiltonian function of the dynamical system for the particle paths. In the present discussion, our interests are in three-dimensional steady flow fields with recirculating path-lines. In the language of dynamical systems, a velocity field possesses recirculating particle paths if the following system of equations is *integrable*:

$$\left.\begin{aligned} \mathrm{d}x(t)/\mathrm{d}t &= u(x(t), y(t), z(t)), \\ \mathrm{d}y(t)/\mathrm{d}t &= v(x(t), y(t), z(t)), \\ \mathrm{d}z(t)/\mathrm{d}t &= w(x(t), y(t), z(t)), \end{aligned}\right\} \tag{3.1}$$

where the steady velocity vector field $\boldsymbol{u} = (u, v, w)$ is known. Following Holm & Kimura (1991), we define integrable in this context to mean that the orbits of (3.1) can be reduced to a parametrized set of non-self-intersecting curves on a two-dimensional manifold. Hence, integrable systems of the form (3.1) possess only periodic and homoclinic or heteroclinic orbits; that is to say all particle paths will be either periodic (recirculating), or they will connect stagnation points. Stated differently, particle paths are level sets of a function on a two-dimensional manifold; they are either recirculating or lie on a curve that contains a fixed point. We remark that in the special case of two-dimensional flow, the two-dimensional manifold of the previous statement is just the plane of the flow and the function on whose level sets the particle paths lie is simply the stream function.

In a truly three-dimensional, steady flow field, the two-dimensional manifold in question may be expressed as the level set of a global function of $\boldsymbol{x} = (x, y, z)$. Hence, particle paths coincide with the intersections of the level sets of *two* functions, which we shall refer to as C and D, both defined globally in the case of recirculating particle paths. One can think of $C(x, y, z) = c$ as defining the two-dimensional manifold, and $D(x, y, z) = d$ as providing the level sets that correspond to orbits on the two-dimensional manifold. Of course, the interpretations of C and D just given may be interchanged. These geometric assertions are equivalent to the mathematical statement

$$\mathrm{d}\boldsymbol{x}(t)/\mathrm{d}t = \boldsymbol{u}(\boldsymbol{x}(t)) = \nabla C \times \nabla D. \tag{3.2}$$

These assertions concerning the geometry of particle paths in three-dimensional flows are well known, where the functions C and D are generally only locally defined. The contribution of Holm & Kimura was to point out that if C and D are globally defined, the geometric statement (3.2) corresponds to an integrable set of ordinary differential equations.

Holm & Kimura pursue the hamiltonian structure of (3.2) by developing a non-canonical Poisson bracket associated with the dynamical system (3.1). The bracket is defined by

$$\{F, G\} \equiv \nabla D \cdot \nabla F \times \nabla G, \tag{3.3a}$$

where F and G are scalar functions of $\boldsymbol{x}$. Using this bracket, one may rewrite the system (3.2) in the hamiltonian form

$$\mathrm{d}\boldsymbol{x}/\mathrm{d}t = \{\boldsymbol{x}, C\}. \tag{3.3b}$$

Note that the roles of C and D may again be interchanged.

In a two-dimensional, steady flow, the stream function is a constant of the motion. In the analogous case in three dimensions, the functions $C(\boldsymbol{x})$ and $D(\boldsymbol{x})$ are both constants of the motion. This may be checked by the simple calculation:

$$\mathrm{d}C(\boldsymbol{x})/\mathrm{d}t = \nabla C \cdot \mathrm{d}\boldsymbol{x}(t)/\mathrm{d}t = \nabla C \cdot \nabla C \times \nabla D = 0,$$

and likewise for D. Moreover, one can make a stronger statement: the two constants of the motion $C(\boldsymbol{x})$ and $D(\boldsymbol{x})$ are *Casimir functions* that correspond to degeneracies of the Poisson bracket (3.3a) (or (3.3a) with C replacing D). By definition a function $K(\boldsymbol{x})$ is a Casimir function of the Poisson bracket (3.3a) if

$$\{K, G\} = 0 \quad \forall G(\boldsymbol{x}).$$

The functions C and D certainly satisfy this property (for the appropriate bracket). For background and examples of non-canonical Poisson brackets and examples of how to find Casimir functions, we refer the interested reader to Holm *et al.* (1985), to Abarbanel *et al.* (1986) and to Szeri & Holmes (1988).

Now we shall extend these results concerning the geometry of the particle paths in the flow by considering a stagnation point of the flow and the nearby flow field. The motive for these investigations is that we shall be interested shortly in the orientation dynamics of particles that follow recirculating paths in the neighbourhood of (elliptic) stagnation points. We shall attempt to derive a result for three-dimensional flows analogous to that derived in §2b.

At a stagnation point $\boldsymbol{x}^*$, we have from equation (3.2) the simple result

$$\mathrm{d}\boldsymbol{x}^*/\mathrm{d}t = \boldsymbol{u}(\boldsymbol{x}^*) = 0 = \nabla C \times \nabla D. \tag{3.4}$$

Geometrically, this result has the following interpretation: at a stagnation point the gradients of the two-dimensional manifolds defined by the level sets of the Casimir functions C and D are co-linear. At a stagnation point of the flow, the surfaces $C(\boldsymbol{x}) = c$ and $D(\boldsymbol{x}) = d$ intersect at a point $\boldsymbol{x}^*$ for the appropriate values c^* and d^*. Equation (3.4) further specifies that the level sets of the Casimir functions C and D are locally parallel near $\boldsymbol{x}^*$. The picture near $\boldsymbol{x}^*$ looks like that sketched in figure 8.

We remark that the particle paths near the fixed point $\boldsymbol{x}^*$ appear on the sketch in figure 8 as the intersections of the level sets of D with the level set of C. We have indicated in figure 8 that these particle paths are (generalized) elliptical curves on the manifold $C = c^*$, as we are presently interested in elliptic stagnation points.

It is not difficult to imagine from the sketch in figure 8, that if the conditions on the Casimir functions and on the surfaces they serve to define (3.4) are valid at the given point $\boldsymbol{x}^*$, then similar statements can be made for some point nearby. In other words, a typical stagnation point in an integrable three-dimensional flow is not isolated. Proof of this statement may be established as follows. The velocity near a stagnation point may be written

$$\boldsymbol{u}(\boldsymbol{x}^* + \delta\boldsymbol{x}) = \nabla \boldsymbol{u}(\boldsymbol{x}^*) \cdot \delta\boldsymbol{x} + O(\|\delta\boldsymbol{x}\|^2). \tag{3.5}$$

This quantity is zero at a point nearby to $\boldsymbol{x}^*$ provided the velocity gradient at $\boldsymbol{x}^*$ has a non-empty null-space. This is checked by computing

$$\det[\nabla \boldsymbol{u}(\boldsymbol{x}^*)] = 0. \tag{3.6}$$

PHILOSOPHICAL TRANSACTIONS OF THE ROYAL SOCIETY A MATHEMATICAL, PHYSICAL & ENGINEERING SCIENCES

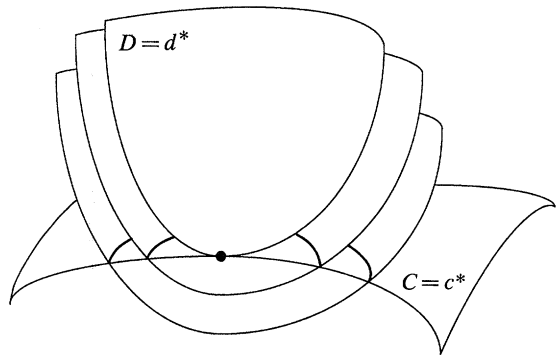

Figure 8. Sketch of the underlying geometrical features of the dynamical system for recirculating particle paths in a three-dimensional flow, in the neighbourhood of an elliptic stagnation point. The surfaces are the level sets of the Casimir functions C and D. The heavy curves are portions of recirculating particle paths in the neighbourhood of the elliptic stagnation point that lie on the 2-manifold $C = c^*$.

In this calculation, which is rather involved, we have made use of the fact that the gradients of the level sets of the Casimir functions are co-linear at the stagnation point $\boldsymbol{x}^*$, i.e. we make use of (3.4). Hence, the stagnation point $\boldsymbol{x}^*$ is not isolated, but is instead a point on a continuous curve of stagnation points. These arguments are essentially an application of the implicit function theorem; we refer the interested reader to Golubitsky & Schaeffer (1985, Appendix 1a) for similar examples.

We have established that three-dimensional flows with recirculating particle paths, free stagnation points $\boldsymbol{x}^*$ are normally points on a stagnation curve that one may write $\boldsymbol{x}^*(s)$. This curve cannot simply end in the fluid. It must end either at a boundary of the fluid, or at a bifurcation point where it branches into two or more stagnation curves. Another possibility is that the stagnation curve is self-intersecting (i.e. closed). We remark that there may be other types of stagnation points, at which there is some degeneracy such as the vanishing of the gradient of a Casimir function. Such points are not covered by the preceding analysis.

(b) *A brief discussion of particle orientation dynamics in three-dimensional flows*

In this section, we give a very brief overview of the arguments of Szeri & Leal (1993) concerning orientation dynamics of particles in three-dimensional flows. In three-dimensional flows, there is no plane in orientation space that is analogous to the plane of the flow when the flow field is two-dimensional. For this reason, it is not possible in three-dimensional flows to decouple the orientation dynamics in the two angular variables one might use to describe the sphere of orientations. Hence for a particle that follows a recirculating path in a three-dimensional flow, the phase space of the differential equation describing the orientation dynamics is not reducible to a torus. We leave the ramifications of this latter statement for §3d, and focus the present discussion on the various types of orientation dynamics that occur in recirculating flow. However, as the dynamics in the two angular variables for the sphere of orientations do not decouple, we shall work in vector notation rather than in orientation angles of the particles.

For the microdynamical equations (1.2), the main results are as follows. The solution of the orientation evolution equation may be obtained conveniently via the equivalent deformation gradient tensor approach; see Bretherton (1962) and also

Table 1. *Orientation dynamics in locally steady, three-dimensional flows*

eigenvalues of $\boldsymbol{\kappa}$	orientation dynamics attractor
$\lambda_1 > \lambda_2 > \lambda_3$	steady, $\parallel \boldsymbol{e}_1$ (eigenvector assoc. with λ_1)
$\lambda_1 > 0$ real, λ_2 and λ_3 complex conjugate	steady, $\parallel \boldsymbol{e}_1$
$\lambda_1 < 0$ real, λ_2 and λ_3 complex conjugate	limit cycle in a plane

Lipscomb *et al.* (1988). We define the *equivalent deformation gradient tensor* $\boldsymbol{Q}$ to be the solution of the linear matrix differential equation

$$\mathrm{d}\boldsymbol{Q}/\mathrm{d}t = \boldsymbol{\kappa}(t)\cdot\boldsymbol{Q}, \quad \boldsymbol{Q}(0) = \boldsymbol{Id}. \tag{3.7}$$

Then the solution of the orientation dynamics problem may be written in terms of $\boldsymbol{Q}$:

$$\boldsymbol{R}(t;\boldsymbol{R}_0) = \boldsymbol{Q}(t)\cdot\boldsymbol{R}_0/\|\boldsymbol{Q}(t)\cdot\boldsymbol{R}_0\|. \tag{3.8}$$

This procedure is valid whether $\boldsymbol{\kappa}$ in the lagrangian frame of the moving particle depends on time or not. Of course, the solution of the nine coupled equations (3.7) may be extremely difficult when these are equations with time-dependent coefficients. Physically, the equivalent deformation gradient tensor $\boldsymbol{Q}(t)$ corresponds to the true deformation gradient tensor between reference ($t = 0$) and current (t) configurations in physical space, but only when the shape factor $G = 1$.

In the very special case of flows that are steady in the lagrangian frame of the moving particle, there are various strong relationships between $\boldsymbol{Q}$ and $\boldsymbol{\kappa}$, that derive from (3.7). For this reason, the orientation dynamics of individual particles may be determined in terms of the equivalent velocity gradient tensor $\boldsymbol{\kappa} = \boldsymbol{\Omega} + G\boldsymbol{E}$. The asymptotic orientation dynamics in the very simple case of (locally) steady flows are completely determined by the eigenvalues and eigenvectors of $\boldsymbol{\kappa}$; the results for generic (i.e. typical) cases are shown in table 1.

Thus, when there is a positive real eigenvalue of $\boldsymbol{\kappa}$, particles simply align with the associated eigenvector. When there is no real, positive eigenvalue of $\boldsymbol{\kappa}$, particles are attracted into the plane of the flow where they rotate *ad infinitum*. Hence, the qualitative nature of the dynamics again depends on the shape factor G.

Our particular interest in the present work concerns particles suspended in flows that are T-periodic in the lagrangian frame associated with the particle. In this case, the right-hand side of equation (1.2) is periodic (non-autonomous) in orientation space. Equation (1.2) may be made autonomous in the standard way, i.e. by appending an additional equation to the system (1.2) of the form $\mathrm{d}\tau/\mathrm{d}t = 1$ and regarding $\boldsymbol{\kappa}$ in (1.2) or (3.7) as a function of τ. The coordinate τ manufactured in this way is regarded as periodic in time. In this way, equation (1.2) may be made autonomous in the phase space formed from the cartesian product of the sphere of orientations and a circle of periodic times τ. Rather than study the continuous-time dynamics in this space, we shall work with the Poincaré map of the sphere of orientations to itself.

The Poincaré map $\mathscr{P}$ is defined by $\mathscr{P}(\boldsymbol{R}_0) = \boldsymbol{R}(t = T;\boldsymbol{R}_0)$. The map has the usual interpretation; one application of the Poincaré map to an initial orientation is equivalent to integration of the differential equation forward for one period, beginning at the initial orientation. The map $\mathscr{P}$ is related to the equivalent deformation gradient tensor $\boldsymbol{Q}$, evaluated at the period of the flow T, by the equation

$$\mathscr{P}(\boldsymbol{R}_0) \equiv \boldsymbol{R}(T;\boldsymbol{R}_0) = \boldsymbol{Q}(T)\cdot\boldsymbol{R}_0/\|\boldsymbol{Q}(T)\cdot\boldsymbol{R}_0\|. \tag{3.9}$$

Table 2. *Orientation dynamics in locally periodic, three-dimensional flows*

eigenvalues of $\boldsymbol{Q}$	orientation dynamics attractor
$\xi_1 > \xi_2 > \xi_3$	limit cycle
$\xi_1 > 1$ real, ξ_2 and ξ_3 complex conjugate	limit cycle
$\xi_1 < 1$ real, ξ_2 and ξ_3 complex conjugate	quasi-periodic attractor (in plane with T-periodic normal)

From (3.9), it is apparent that fixed points of the Poincaré map $\boldsymbol{R}_T$ correspond to time-periodic solutions of the underlying differential equation; thus $\boldsymbol{R}(t+T;\, \boldsymbol{R}_T) = \boldsymbol{R}(t;\, \boldsymbol{R}_T)$. Moreover, fixed points $\boldsymbol{R}_T$ can be shown to be eigenvectors of the equivalent deformation gradient tensor $\boldsymbol{Q}$, evaluated at the period of the flow T, with corresponding eigenvalue $\|\boldsymbol{Q}(T)\cdot\boldsymbol{R}_T\|$.

Hence, in flows that are time-periodic in the lagrangian frame of the moving particle, the orientation dynamics are completely determined by the eigenvalues and eigenvectors of the equivalent deformation gradient tensor $\boldsymbol{Q}(T)$, which is the solution of equation (3.7). The results for generic cases are summarized in table 2.

When the equivalent deformation gradient tensor $\boldsymbol{Q}(T)$ has a real eigenvalue greater than one, the corresponding attractor for the orientation dynamics is periodic. The eigenvector associated with the real eigenvalue greater than one is the instantaneous orientation of the attractor at $t = 0,\ T,\ 2T,\ \ldots$. The integral curve of the attractor over the period may be reconstructed by use of equation (3.8) and the time-dependent equivalent deformation gradient tensor.

When the equivalent deformation gradient tensor $\boldsymbol{Q}(T)$ has no real eigenvalue greater than one, then one can show that the Poincaré map (3.9) possesses an attracting invariant plane. In other words, particles are mapped closer and closer into the invariant plane over each period T. Once they lie in the invariant plane, particles simply rotate around within the invariant plane. The combination of periodic rotation in the invariant plane, and periodic motion around the recirculating particle path is equivalent to quasi-periodic orientation dynamics in the lagrangian frame. If the origin of time were shifted, with a corresponding shift in the initial condition of equation (3.7) and in the Poincaré map (3.9), one would find a different attracting invariant plane of the Poincaré map. Thus the quasi-periodic attractor in the lagrangian frame corresponds to an attracting invariant plane with a T-periodic normal in the eulerian frame, as shown in the sketch in figure 9.

At a fixed location, within the invariant plane, particles simply rotate at a varying speed. This leads to a new type of fixed pattern when the (orientation dynamics) attractor is quasi-periodic: at each fixed location along the associated particle path, all particles lie in a plane with normal that changes smoothly along the particle path.

Thus, in three-dimensional, steady recirculating flows of suspensions, there are two types of fixed patterns. At a fixed location in space all the particles may be aligned with a steady orientation, or they may all be rotating but co-planar. These situations correspond to periodic and quasi-periodic attractors in the lagrangian sense, respectively. Moreover, there are no non-patterned regions of the flow when it is three-dimensional. The type of attractor associated with the orientation dynamics depends on the shape factor G.

PHILOSOPHICAL TRANSACTIONS OF THE ROYAL SOCIETY A MATHEMATICAL, PHYSICAL & ENGINEERING SCIENCES

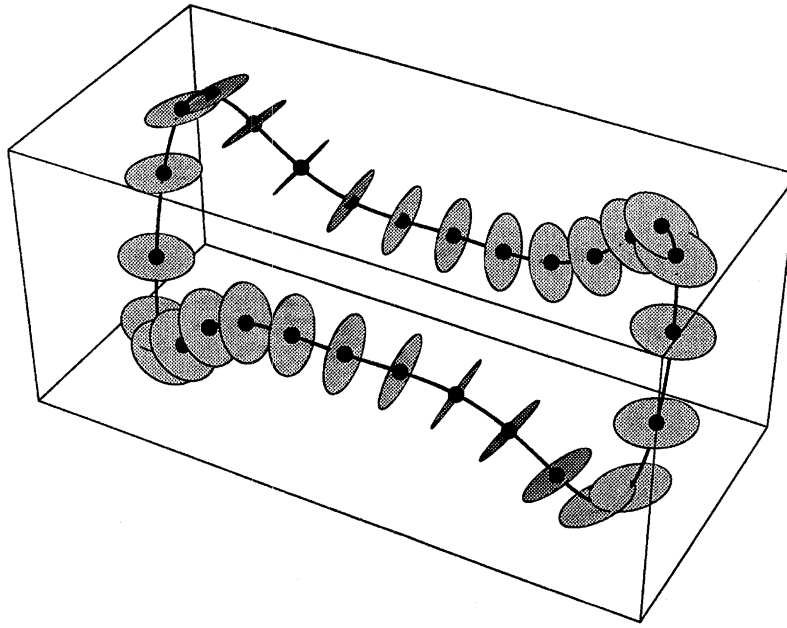

Figure 9. Sketch of the attracting invariant planes in the eulerian reference frame for the orientation dynamics of particles following a recirculating path through physical space. The asymptotic orientation dynamics of individual particles is characterized by a quasi-periodic attractor in the lagrangian frame.

(*c*) *Conditions that apply near an elliptic stagnation curve*

We analyse the particle paths and orientation dynamics in the neighbourhood of an elliptic stagnation point on a stagnation curve in a three-dimensional flow, as we did in two dimensions in §2*b*. We chose local cartesian coordinates so that the null space of the velocity gradient tensor is span $\{(1, 0, 0)\}$. Thus, the stagnation curve continues, locally, in the $\pm(1, 0, 0)$ directions. Hence, the local gradients of the level sets of the Casimir functions are in the directions $\pm(1, 0, 0)$.

By use of Schur's theorem, one can write the velocity gradient tensor evaluated at an elliptic stagnation point in the form

$$\nabla \boldsymbol{u}(\boldsymbol{x}^*) = \begin{bmatrix} 0 & \alpha & \beta \\ 0 & 0 & \lambda \\ 0 & -\lambda & 0 \end{bmatrix}, \tag{3.10}$$

where α, β and $\lambda > 0$ are real. The particle paths near $\boldsymbol{x}^*$ are solutions of

$$\mathrm{d}\delta\boldsymbol{x}/\mathrm{d}t = \nabla \boldsymbol{u}(\boldsymbol{x}^*) \cdot \delta\boldsymbol{x},$$

which may easily be computed in coordinates:

$$\begin{bmatrix} \delta x_1(t) \\ \delta x_2(t) \\ \delta x_3(t) \end{bmatrix} = \begin{bmatrix} \delta x_1(0) + \lambda^{-1}[\alpha\,\delta x_2(0) + \beta \delta x_3(0)] \sin \lambda t + \lambda^{-1}[\alpha\,\delta x_3(0) - \beta\,\delta x_2(0)](1 - \cos \lambda t) \\ \delta x_2(0) \cos \lambda t + \delta x_3(0) \sin \lambda t \\ \delta x_3(0) \cos \lambda t - \delta x_2(0) \sin \lambda t \end{bmatrix}. \tag{3.11}$$

Note that these particle paths are periodic with period $T_{\mathrm{path}} = 2\pi/\lambda$.

The orientation dynamics, on the other hand, evolve according to the equivalent velocity gradient tensor

$$\boldsymbol{\kappa}(\boldsymbol{x}^* + \delta\boldsymbol{x}(t)) = \boldsymbol{\kappa}(\boldsymbol{x}^*) + \ldots, \tag{3.12}$$

which is computed in the same coordinates to leading order

$$\boldsymbol{\kappa}(\boldsymbol{x}^*) = \begin{bmatrix} 0 & \frac{1}{2}(G+1)\,\alpha & \frac{1}{2}(G+1)\,\beta \\ \frac{1}{2}(G-1)\,\alpha & 0 & \lambda \\ \frac{1}{2}(G-1)\,\beta & -\lambda & 0 \end{bmatrix}. \tag{3.13a}$$

To leading order then, $\boldsymbol{\kappa}$ is steady, with eigenvalues

$$0, \pm\tfrac{1}{2}[(G^2-1)\,(\alpha^2+\beta^2) - 4\lambda^2]^{\frac{1}{2}}, \tag{3.13b}$$

i.e. 0 and a complex-conjugate pair (for $G \leqslant 1$). This corresponds to the following dynamics: all orientations are periodic and the orientation (1, 0, 0) is an elliptic (degenerate) equilibrium orientation. In other words, *there is no attractor*. Note that this case is not present in table 1 which pertains to particles in flows that are steady in the lagrangian frame; the reason is that this case in which there is a zero eigenvalue is not generic. In particular, Szeri & Leal (1993) have shown that this situation is degenerate. If one were to include the next term in the approximation

$$\boldsymbol{\kappa}(\boldsymbol{x}^* + \delta\boldsymbol{x}(t)) = \boldsymbol{\kappa}(\boldsymbol{x}^*) + \nabla\boldsymbol{\kappa}(\boldsymbol{x}^*)\cdot\delta\boldsymbol{x}(t)\ldots, \tag{3.14}$$

the orientation dynamics would be qualitatively different; either there would be a periodic attractor, or there would be a quasi-periodic attractor in general. A periodic attractor would be of period $T_{\text{orient}} = 2\pi/\lambda$, the same period as that of the particle paths. Thus, there would be a steady pattern of attracting orientations of particles near the stagnation point, after the decay of initial transients. A quasi-periodic attractor would have an associated invariant plane with a normal that is periodic with period $T_{\text{normal}} = 2\pi/\lambda$, the same period as that of the particle paths. Thus, there would be a steady pattern of attracting planes near the stagnation point, after the decay of initial transients.

However, in order to discern which possibility will be the case, one must solve the second-order problem for the orientation dynamics. This does not seem to be practical. In summary, our study of the orientation dynamics of particles near an elliptic stagnation point is inconclusive. In this connection, it is worth noting that in the example problem of §3*e*, we observe a zone of quasi-periodic particle orientation dynamics in the neighbourhood of every elliptic stagnation point.

(*d*) *Structure of patterned zones*

There is an important difference between the structure of patterned zones in two-dimensional and three-dimensional flows of suspensions. This difference, to which we have already alluded, pertains to the phase space of the differential equation for orientation dynamics of particles that follow recirculating path-lines. In two dimensions, the phase space is reducible to a torus, i.e. to the product of a circle (for orientation angle in the plane) and a circle (for periodic time). As we saw in §2, there may be interesting, observable effects that derive from the different homotopy classes to which different periodic attractors may belong. In particular, we saw that bands of quasi-periodic orientation dynamics must separate two patterned zones in the same recirculating cell that are characterized by a different number of flips per circuit.

PHILOSOPHICAL TRANSACTIONS OF THE ROYAL SOCIETY A MATHEMATICAL, PHYSICAL & ENGINEERING SCIENCES

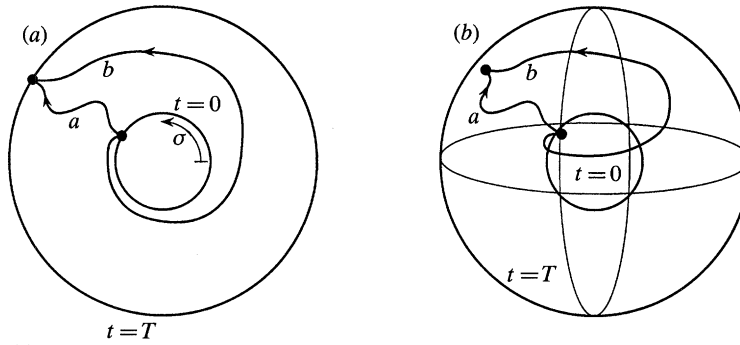

Figure 10. (*a*) Sketch to accompany the discussion of homotopy classes of periodic attractors for the orientation dynamics. In two-dimensional recirculating flows, the reduced phase space for orientation dynamics is a torus, here represented as an annulus with the circles $t = 0$ and $t = T$ identified. The two periodic attractors labelled a and b belong to different homotopy classes, corresponding physically to a different number of end-over-end flips of the particle per circumnavigation of the particle path. (*b*) Same as (*a*), but for three-dimensional flows, in which the phase space for orientation dynamics is not reducible from the cartesian product of a sphere and a circle. The periodic attractors labelled a and b belong to the same homotopy class in this case; a can be smoothly deformed into b.

As a prelude to our considerations of three-dimensional flows, let us investigate the phase space for two-dimensional flows in somewhat greater detail. To begin, consider the sketch in figure 10*a*.

In figure 10*a*, we have a representation of the (σ, t) torus as an annulus, with edges $t = 0$ and $t = T$ identified. There is one such annulus associated with each recirculating particle path in the flow. The reason for working with this geometric representation of the phase space is to simplify conceptually the extension to the appropriate phase space for three-dimensional recirculating flows. We emphasize, however, that our analysis applies to two-dimensional flows in which suspended particles are free to rotate out of the plane of the flow. It is only as a consequence of the decoupling of orientation dynamics in two orientation angles that we may consider the reduced phase space as described. A periodic attractor must have $\sigma(T;\ \sigma_0) = \sigma_0$, by definition; hence the initial and final conditions must lie on a $\sigma =$ constant ray ($\sigma = \sigma_0$) in this representation. In figure 10*a* we show two possible periodic attractors associated with a recirculating particle path. The two possible periodic attractors a and b in figure 10*a*, with $n(a) = 0$ and $n(b) = 1$ belong to different homotopy classes. One cannot smoothly deform a into b and maintain the restriction $\sigma(T;\ \sigma_0) = \sigma_0$. Different homotopy classes of attractors are associated, physically, with different numbers of end-over-end flips of the particles as they circumnavigate their particle paths in physical space. It is this curious topological restriction that leads to the thin quasi-periodic bands separating patterned zones characterized by different numbers of end-over-end flips.

Now, in three dimensional flows, the phase space for the orientation dynamics problem along recirculating particle paths cannot be reduced from the cartesian product of a sphere (of orientations) and a circle (of periodic time), as the velocity gradient tensor is fully three-dimensional. The ramifications for pattern formation are as follows. In figure 10*b*, we show a sketch of phase space represented as the space between two concentric spheres labelled $t = 0$ and $t = T$, which are identified. Thus, a periodic attractor emanates from a point on the sphere $t = 0$ and proceeds to the point on the same ray on the sphere $t = T$. Clearly, the two possible periodic

attractors labelled a and b in figure 10b are in the same homotopy class, as one can deform a smoothly into b, and yet maintain the topological restriction regarding periodicity.

Hence, in three-dimensional recirculating flows of suspensions, we do not have phenomena analogous to flip numbers or to thin quasi-periodic bands separating patterned zones with different flip numbers. Instead, in three-dimensional recirculating flows of suspensions, the are two states of the flowing suspension: one state has the particles everywhere locally aligned along a single preferred orientation, and the other state consists of particles locally rotating in preferred planes of orientations.

(e) *Example: flow within a fluid drop in a linear external flow field*

Now we move on to an example of a three-dimensional recirculating flow to see how the structures we have identified may arise. We consider the Stokes flow within a neutrally buoyant, spherical drop driven by an external flow of the surrounding fluid. This flow has been examined recently by Stone *et al.* (1991) in the context of chaotic particle paths, which may or may not exist depending on the external flow; see also the recent work of Bajer & Moffatt (1990). We are interested in the sub-class of these flows in which the particle paths are recirculating (and hence, not chaotic).

The external flow that drives the internal flow is steady and linear. As such, this flow is characterized by a steady rate-of-strain tensor $\boldsymbol{E}$ and vorticity vector $\boldsymbol{\omega}$. The velocity field within the drop that arises in response to the external flow is developed in Stone *et al.* (1991):

$$\boldsymbol{u}(\boldsymbol{x}) = \frac{1}{2(1+\lambda)}[(5r^2-3)\,\boldsymbol{E}\cdot\boldsymbol{x} - 2(\boldsymbol{x}\cdot\boldsymbol{E}\cdot\boldsymbol{x})\,\boldsymbol{x}] + \tfrac{1}{2}\boldsymbol{\omega}\times\boldsymbol{x}. \tag{3.15}$$

In this expression, lengths have been non-dimensionalized with respect to the drop radius a; the velocity has been non-dimensionalized with respect to $\mathscr{G}a$ where $\mathscr{G}$ is a typical shear rate of the external flow. λ is the viscosity ratio of the inner fluid over the outer fluid, and $r^2 = \boldsymbol{x}\cdot\boldsymbol{x}$. We consider here the subset of external flows without vorticity, i.e. $\boldsymbol{\omega} = 0$. Time may be re-scaled so that the particle path equations may be written

$$\mathrm{d}\boldsymbol{x}(t)/\mathrm{d}t = \boldsymbol{u}(\boldsymbol{x}(t)) = (5r^2-3)\,\boldsymbol{E}\cdot\boldsymbol{x} - 2(\boldsymbol{x}\cdot\boldsymbol{E}\cdot\boldsymbol{x})\,\boldsymbol{x}. \tag{3.16}$$

As a particular example flow, we focus on the case where the rate-of-strain tensor in its eigenbasis has the form

$$\boldsymbol{E} = \begin{bmatrix} 1 & 0 & 0 \\ 0 & 2 & 0 \\ 0 & 0 & -3 \end{bmatrix}. \tag{3.17}$$

Then, after a rather involved calculation beginning from the geometric form of the particle path equations (3.2), one can find the Casimir functions C and D:

$$C(\boldsymbol{x}) = x^5/y^4z, \quad D(\boldsymbol{x}) = (y^5z^2/x^4)\,(1-x^2-y^2-z^2). \tag{3.18a}$$

Equation (3.2) may be verified. We remark that the Casimirs C and D were actually found by working in standard spherical polar coordinates (ρ, θ, ϕ) and searching for separable forms for C and D that yield equation (3.2). In standard spherical polar coordinates, C and D have the form:

$$\left.\begin{aligned} C(\rho,\theta,\phi) &= \tan\theta\cot^4\phi\cos\phi, \\ D(\rho,\theta,\phi) &= r^3(1-r^2)\sin\theta\cos^2\theta\tan^4\phi\sin\phi. \end{aligned}\right\} \tag{3.18b}$$

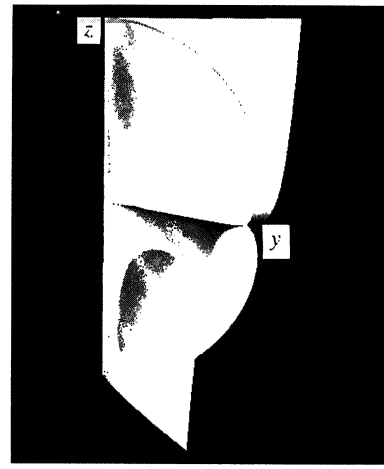

Figure 11. Intersection of the level sets of the Casimir functions C and D with $c = 0.01$ and $d = 1$, in the domain $y \geqslant 0$. The surface associated with C is the warped sheet, and the surface associated with D is the closed bean-shaped surface. The recirculating particle paths in this flow follow the intersections of the level sets of C and D.

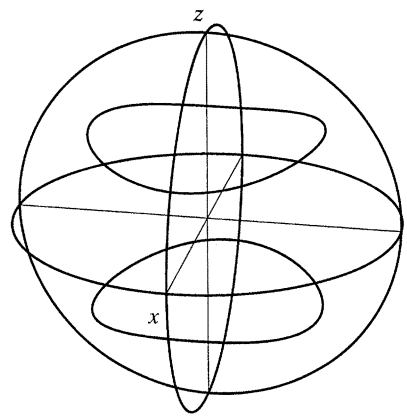

Figure 12. The two closed curves of elliptic stagnation points given parametrically by equation (3.19), for a spherical drop suspended in the steady, linear, external flow (3.17). There is another ring of stagnation points that lies in the x–y plane on the circle with unit radius (the equator), and a pair of degenerate stagnation points at the poles.

In figure 11 we show the intersection of the level sets of the two Casimir functions C and D; the intersection shown thus corresponds to a recirculating particle path.

There are two fully three-dimensional, closed curves of elliptic stagnation points, given parametrically over $0 \leqslant \phi < 2\pi$ by

$$(x^*(\phi),\, y^*(\phi),\, z^*(\phi)) = \frac{1}{\sqrt{5}}\left(\frac{(3\sqrt{2})\cos\phi}{(9-\cos 2\phi)^{\frac{1}{2}}},\, \frac{(3\sqrt{2})\sin\phi}{(9-\cos 2\phi)^{\frac{1}{2}}},\, \frac{\pm(\sqrt{3})\,(2-\cos^2\phi)^{\frac{1}{2}}}{(5-\cos^2\phi)^{\frac{1}{2}}}\right). \tag{3.19}$$

These curves are shown in figure 12.

Now that we have cast light on the particle paths in the flow field within the spherical drop, we move on to consider the asymptotic orientation dynamics. Owing

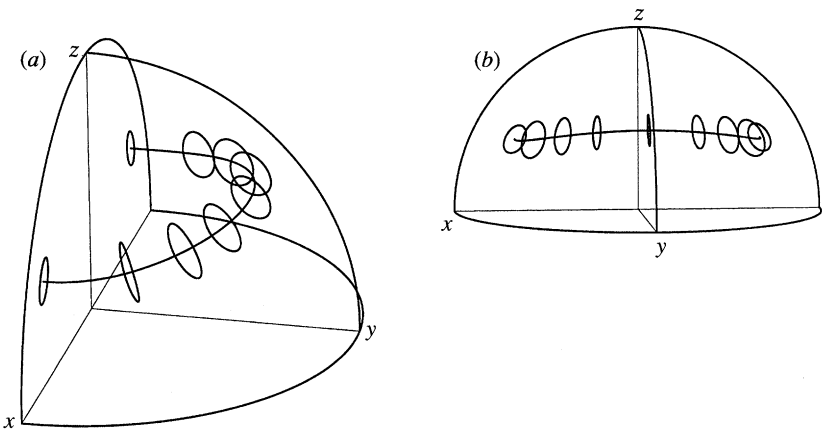

Figure 13. (*a*) Pattern boundary between the two zones of the flowing suspension that coexist in the example flow of §3. The two zones are those associated with periodic and with quasi-periodic particle orientation dynamics in the lagrangian frame. The closed curves lie on the pattern boundary; they correspond to particle paths at the sharp transition between periodic orientation dynamics outside the (imaginary) surface, and quasi-periodic orientation dynamics within the surface. The other curve passing through the closed particle paths corresponds to the curve of elliptic stagnation points. (*b*) Same as (*a*), but from a different point of view.

to symmetries of the external flow field, it is sufficient to consider one quarter of the spherical drop; we choose to concentrate on the domain

$$\mathscr{D} = \{(x, y, z) : x^2 + y^2 + z^2 \leqslant 1, y \geqslant 0, z \geqslant 0\}.$$

In order to investigate the asymptotic particle dynamics, we proceed as follows. First, we choose an initial point in the flow field and integrate the particle path over one period back to the initial point. Next, we integrate the evolution equation for the equivalent deformation gradient tensor $\boldsymbol{Q}$, equation (3.7), over one period of the flow. This allows us to assemble the Poincaré map (3.9). The eigenvalues of $\boldsymbol{Q}$ provide the information on the nature of the attractor for the orientation dynamics, as presented in table 2. The attractor is either periodic or it is quasi-periodic. If the attractor is periodic, then the eigenvector associated with the maximum (real) eigenvalue provides an initial condition for the periodic attractor. This orientation can be 'integrated' around the particle path by use of the time-dependent tensor $\boldsymbol{Q}$ and equation (3.8).

If, instead, the attractor is quasi-periodic, then we must find the invariant planes at each fixed location along the closed particle path. This is done as follows. For each fixed location of interest along the particle path, we integrate equation (3.7) beginning at $t = 0$ over one period of the flow. The resulting tensor $\boldsymbol{Q}$ will yield a plane in orientation space that is invariant under the transformation (3.9). The normal to this plane $\boldsymbol{n}$ is easily computed from the equations

$$\boldsymbol{n} \cdot \boldsymbol{u} = 0, \quad \boldsymbol{n} \cdot \boldsymbol{Q}(T) \cdot \boldsymbol{u} = 0, \quad |\boldsymbol{u}| = 1.$$

These procedures have been carried out for the flow field interior to the drop (3.15), with zero vorticity and rate-of-strain tensor (3.17), and for particles with shape factor $G = 0.9$. The results we have obtained fall into the following broad description. On those particle paths that begin sufficiently close to the elliptic stagnation curve, the particle dynamics are quasi-periodic. This result recalls the two-dimensional example of §2, where we found quasi-periodic dynamics occurring in the regions

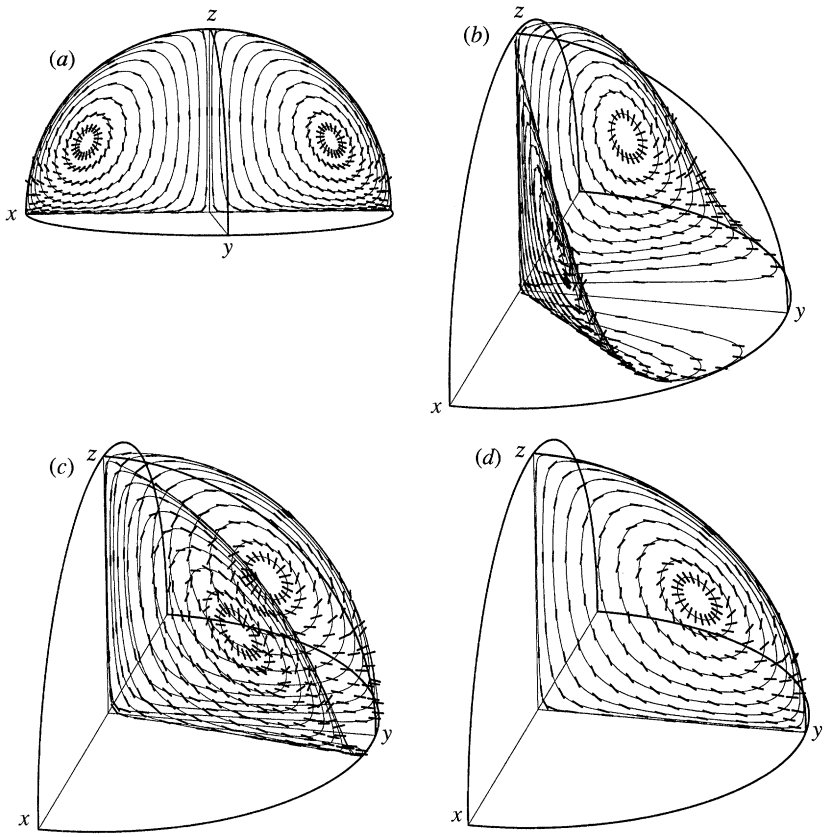

Figure 14. (*a*) Particle paths and associated attractors in the periodic zone outside the pattern boundary shown in figure 13. The initial points of the particle paths were taken on the plane $y = 0$, on a ray from the origin to the elliptic point in the plane, with the innermost recirculating paths lying just outside the pattern boundary. (*b*) Particle paths and associated attractors in the periodic zone outside the pattern boundary shown in figure 13. The initial points of the particle paths were taken on the plane $y = \pm\frac{1}{2}x$, on a ray from the origin to the elliptic point in the plane, with the innermost recirculating paths lying just outside the pattern boundary. (*c*) Particle paths and associated attractors in the periodic zone outside the pattern boundary shown in figure 13. The initial points of the particle paths were taken on the plane $y = \pm 2x$, on a ray from the origin to the elliptic point in the plane, with the innermost recirculating paths lying just outside the pattern boundary. (*d*) Particle paths and associated attractors in the periodic zone outside the pattern boundary shown in figure 13. The initial points of the particle paths were taken on the plane $x = 0$, on a ray from the origin to the elliptic point in the plane, with the innermost recirculating paths lying just outside the pattern boundary.

surrounding the elliptic stagnation points. (However, recall that our analytical efforts at proving that this must be the case in three-dimensional flows were inconclusive.) On those particle paths that lie further from the elliptic stagnation curve, the particle dynamics are periodic. In figure 13, we show bounding particle paths on the (imaginary) surface that separates these two distinct patterned zones.

The imaginary surface shown in figure 13 is the *pattern boundary* between the two different zones that coexist in this example flow: those associated with periodic and with quasi-periodic particle dynamics.

Outside the pattern boundary shown in figure 13, the particle dynamics are periodic, corresponding to a fixed pattern of attracting orientations in the Eulerian

PHILOSOPHICAL TRANSACTIONS OF THE ROYAL SOCIETY A MATHEMATICAL, PHYSICAL & ENGINEERING SCIENCES

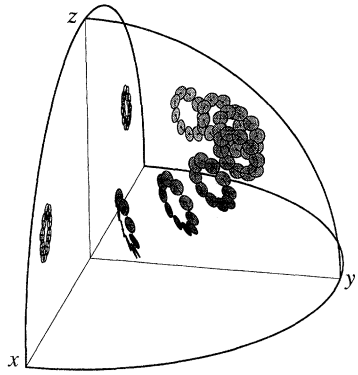

Figure 15. Particle paths and associated attracting planes in the quasi-periodic zone just inside the pattern boundary shown in figure 13.

reference frame. In figure 14, we show plots of the fixed pattern associated with the periodic particle dynamics along various sheets of recirculating particle paths outside the pattern boundary. The first sheet of recirculating particle paths (figure 14*a*) happens to lie in the x–z plane of the flow, which is a plane of symmetry of the flow field; the last sheet of recirculating particle paths (figure 14*d*) lies in the y–z plane of the flow, which is another plane of symmetry of the flow field.

The particles that follow the outermost recirculating paths in each of the figures are, for the most part, quite closely aligned with the tangent to the particle path, with the exception of the region of the flow near the equator of the spherical drop. There, the pattern of particle orientations is nearly normal to the particle path. The particles are less aligned with the tangent to the particle path as one moves inward in the set(s) of recirculating paths shown in each diagram. The innermost recirculating path shown in each of figure 14*a*–*d* is a path just outside the pattern boundary where the transition to quasi-periodic particle dynamics takes place. It is interesting to note that on this limiting particle path, the particles are arranged in a way that is almost perpendicular to the tangent to the particle path everywhere.

The quasi-periodic zone occurs in the present example within the pattern boundary indicated in figure 13. In figure 15, we show the fixed inclinations of the attracting invariant planes of particle orientations at various stages along the particle paths that lie just inside the pattern boundary shown in figure 13.

One observes that the pattern of attracting planes varies smoothly throughout the part of the flow that is characterized by quasi-periodic dynamics. In the places where the pattern boundary cuts the x–z or y–z plane, and the particle path lies is a plane owing to symmetry, the invariant planes of the particle orientation dynamics lie also in the same planes.

In summary, this three-dimensional example flow of a suspension of orientable particles has shown the principal features of pattern formation that we have described. These features included: (i) a strongly ordered state characterized by attracting orientations of particles that are fixed in the eulerian frame; (ii) a weakly ordered state characterized by attracting planes of orientations of particles that are fixed in the eulerian frame; (iii) smooth spatial variation in the two types of patterns; and (iv) a sharp boundary between different types of patterns.

PHILOSOPHICAL TRANSACTIONS OF THE ROYAL SOCIETY A MATHEMATICAL, PHYSICAL & ENGINEERING SCIENCES

4. Conclusions

We have investigated in detail the steady, recirculating flows of suspensions of orientable particles in two and in three dimensions. After the decay of initial transients, the orientations of individual suspended particles in these flows are governed by the global attractors for the orientation dynamics. The patterns that arise are associated with the smoothly varying attractors for the orientation dynamics. Hence, the organized behaviour develops in response to the flow itself. The flow creates the order, maintains the order, and gives the material its characteristic disposition of suspended particles. If the flow were to cease, brownian motions would eventually erase the organized behaviour.

The behaviour of each particle is determined only by the history of the local flow fields it has experienced. We have shown that regularity of solutions to ordinary differential equations allows one to synthesize a coherent picture of which orientations are favoured over regions of the flow, by a consideration of the variation of attractors for the orientation dynamics across particle paths in the flow.

In two-dimensional flows, the important features one may observe include: (i) zones of quasi-periodic particle dynamics surrounding elliptic stagnation points in the flow (a disordered state); (ii) zones of steady patterns of fixed attracting orientations that vary smoothly across particle paths (an ordered state); (iii) a like number of end-over-end flips of particles in the same patterned zone; and (iv) thin, quasi-periodic bands separating patterned zones with distinct flip numbers. In three-dimensional flows, the important features are somewhat different: (i) there are two states of the material that may co-exist side by side, associated with periodic and with quasi-periodic attractors in the lagrangian frame; and (ii) there are no phenomena analogous to the shared flip number of particles in a zone or to thin quasi-periodic bands separating zones of different flip number. Because the dynamical behaviour of particles in a recirculating, three-dimensional flow field are structurally stable, one can expect that small perturbations due to slight particle flexibility or weak brownian motions or minute particle–particle interactions would not change the qualitative nature of the patterns we have described. In addition, we note that Gañán-Calvo & Lasheras (1991) have shown that particles may still follow a recirculating path through a flow-field even though they do not follow the same trajectories as fluid particles. Hence pattern formation may also be of importance for particles with dynamical effects.

Finally, it is interesting to speculate on what may be the uses of the new phenomena we have described. The principal use one might imagine would be in the field of material processing. We have already pointed out that the phenomena we have described are purely kinematical, and therefore occur in flows of suspensions whether or not the particles affect the macroscopic flow. It is also interesting to note that these phenomena are unaffected by a change in the viscosity provided that the flow field is preserved, geometrically, under changes in the viscosity. This latter condition is satisfied in a Stokes flow.

One could imagine a materials processing operation in which a composite material is the described product. In the liquid phase, pattern formation might be used in order to produce desired patterns of the distribution of particle orientations through the part *that survive intact as the material hardens*. These ideas might be applied to the manufacture of plastic parts, in which the flow that induces the pattern formation would be driven by motion of the boundary or by convection effects. In this case, the

suspended phase might be included for its strengthening or its optical properties, depending on the application. Another interesting use for these phenomena occurs if the suspending phase is a metal. In this case, the principles of electromagnetic stirring might be applied to engineer any desired pattern of stirring and patterns of orientation of the suspended phase, to produce a composite material with desired properties. We refer the reader to the interesting paper by Moffatt (1991) for background on electromagnetic stirring.

The author thanks Mr Vi Vuong and Dr Alan Schiano for assistance in the preparation of figure 11. In addition, the author is grateful to Professor Frank Park for a brief but helpful discussion on the homotopy classes of closed curves on a two-dimensional torus, to Professor Gary Leal for the encouragement to pursue this work, and to Dr Ulises González for his careful reading of the manuscript and helpful comments. This research was supported in part by the University of California, Irvine through an allocation of computer resources.

References

Abarbanel, H. D. I., Holm, D. D., Marsden, J. E. & Ratiu, T. S. 1986 Nonlinear stability analysis of stratified fluid equilibria. *Phil. Trans. R. Soc. Lond.* A **318**, 349–409.

Arnold, V. I. 1988 *Geometrical methods in the theory of ordinary differential equations*. Springer.

Bajer, K. & Moffatt, H. K. 1990 On a class of steady confined Stokes flows with chaotic streamlines. *J. Fluid Mech.* **212**, 337–363.

Bretherton, F. P. 1962 The motion of rigid particles in a shear flow at low Reynolds number. *J. Fluid Mech.* **14**, 284–304.

Frattini, P. L. & Fuller, G. G. 1986 Rheo-optical studies of the effect of weak Brownian rotations in sheared suspensions. *J. Fluid Mech.* **168**, 119–150.

Gañán-Calvo, A. M. & Lasheras, J. C. 1991 The dynamics and mixing of small spherical particles in a plane, free shear layer. *Phys. Fluids* A **3**, 1207–1217.

Golubitsky, M. & Schaeffer, D. G. 1985 *Singularities and groups in bifurcation theory*. Springer.

Holm, D. D. & Kimura, Y. 1991 Zero-helicity Lagrangian kinematics of three-dimensional advection. *Phys. Fluids* A **3**, 1033–1038.

Holm, D. D., Marsden, J. E., Ratiu, T. S. & Weinstein, A. 1985 Nonlinear stability of fluid and plasma equilibria. *Phys. Rep.* **123**, 1–116.

Jeffery, G. B. 1922 The motion of ellipsoidal particles immersed in a fluid. *Proc. R. Soc. Lond.* A **102**, 161–179.

Lipscomb, G. G., Denn, M. M., Hur, D. U. & Boger, D. V. 1988 The flow of fiber suspensions in complex geometries. *J. non-newt. Fluid Mech.* **26**, 297–325.

Moffatt, H. K. 1991 Electromagnetic stirring. *Phys. Fluids* A **3**, 1336–1343.

Stone, H. A., Nadim, A. & Strogatz, S. H. 1991 Chaotic streamlines inside drops immersed in steady Stokes flows. *J. Fluid Mech.* **232**, 629–646.

Szeri, A. J. & Holmes, P. J. 1988 Nonlinear stability of axisymmetric swirling flows. *Phil. Trans. R. Soc. Lond.* A **326**, 327–354.

Szeri, A. J. & Leal, L. G. 1993 Microstructure suspended in three-dimensional flows. *J. Fluid Mech.* **250**, 143–167.

Szeri, A. J., Milliken, W. J. & Leal, L. G. 1992 Rigid particles suspended in time-dependent flows: irregular vs. regular motion, disorder vs. order. *J. Fluid Mech.* **237**, 33–56.

Szeri, A. J., Wiggins, S. W. & Leal, L. G. 1991 On the dynamics of microstructure in unsteady, spatially inhomogeneous, two-dimensional fluid flows. *J. Fluid Mech.* **228**, 207–241.

Received 2 March 1992; revised 29 September 1992; accepted 20 January 1993

PHILOSOPHICAL TRANSACTIONS OF THE ROYAL SOCIETY A MATHEMATICAL, PHYSICAL & ENGINEERING SCIENCES

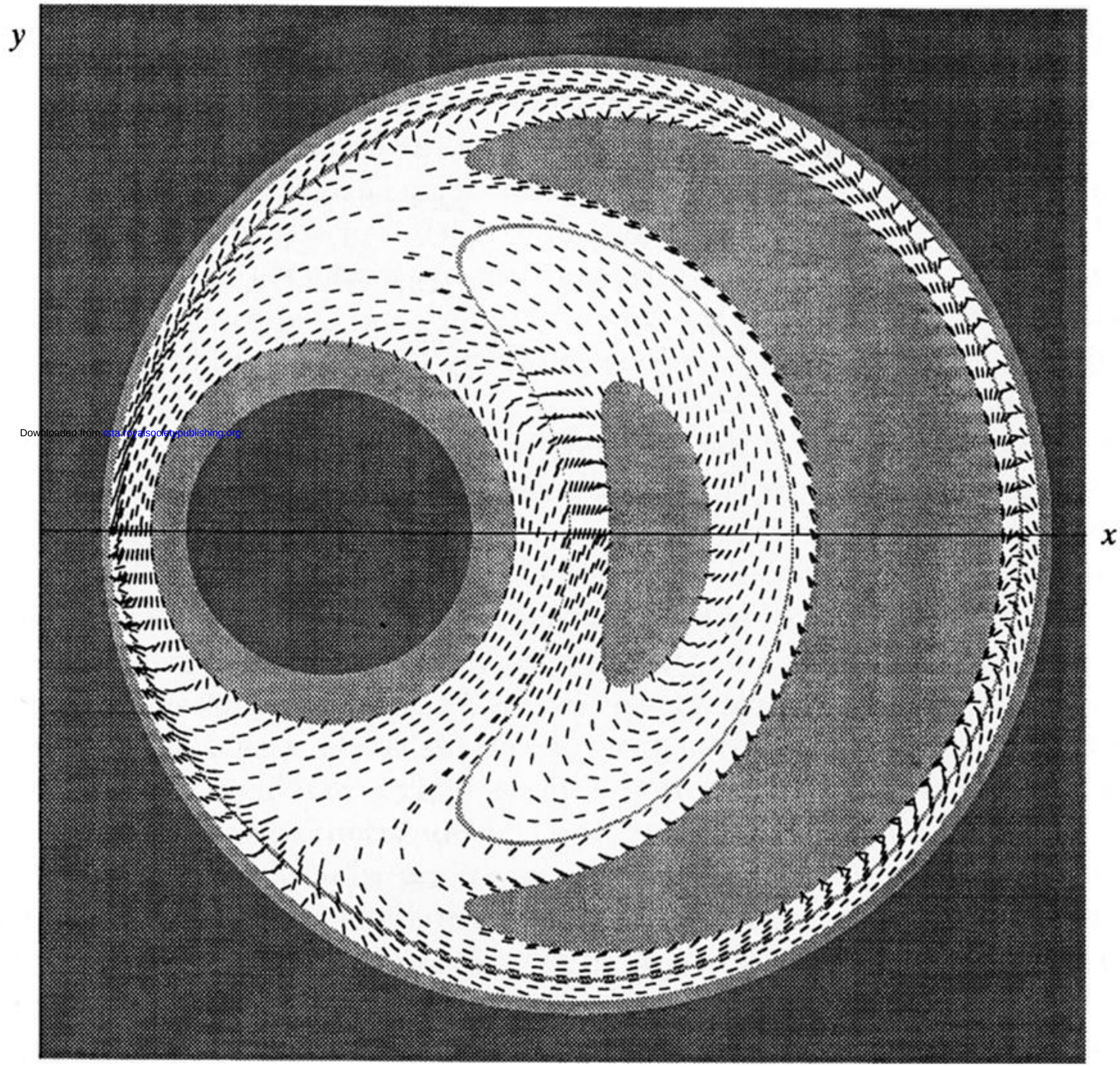

Figure 5. Overview of the example in §2, in which particles ($G = 0.9$) are suspended in the steady flow between eccentric, co-rotating cylinders (dark grey). The counter-clockwise speeds of rotation of the cylinders are (inner) 20 and (outer) 1. The directors indicate the attractors in patterned zones; light grey zones are characterized by quasi-periodic dynamics. The four recirculating regions are denoted A (just within the outer cylinder), B (around the inner cylinder), and C and D, to the right of the inner cylinder, left to right.

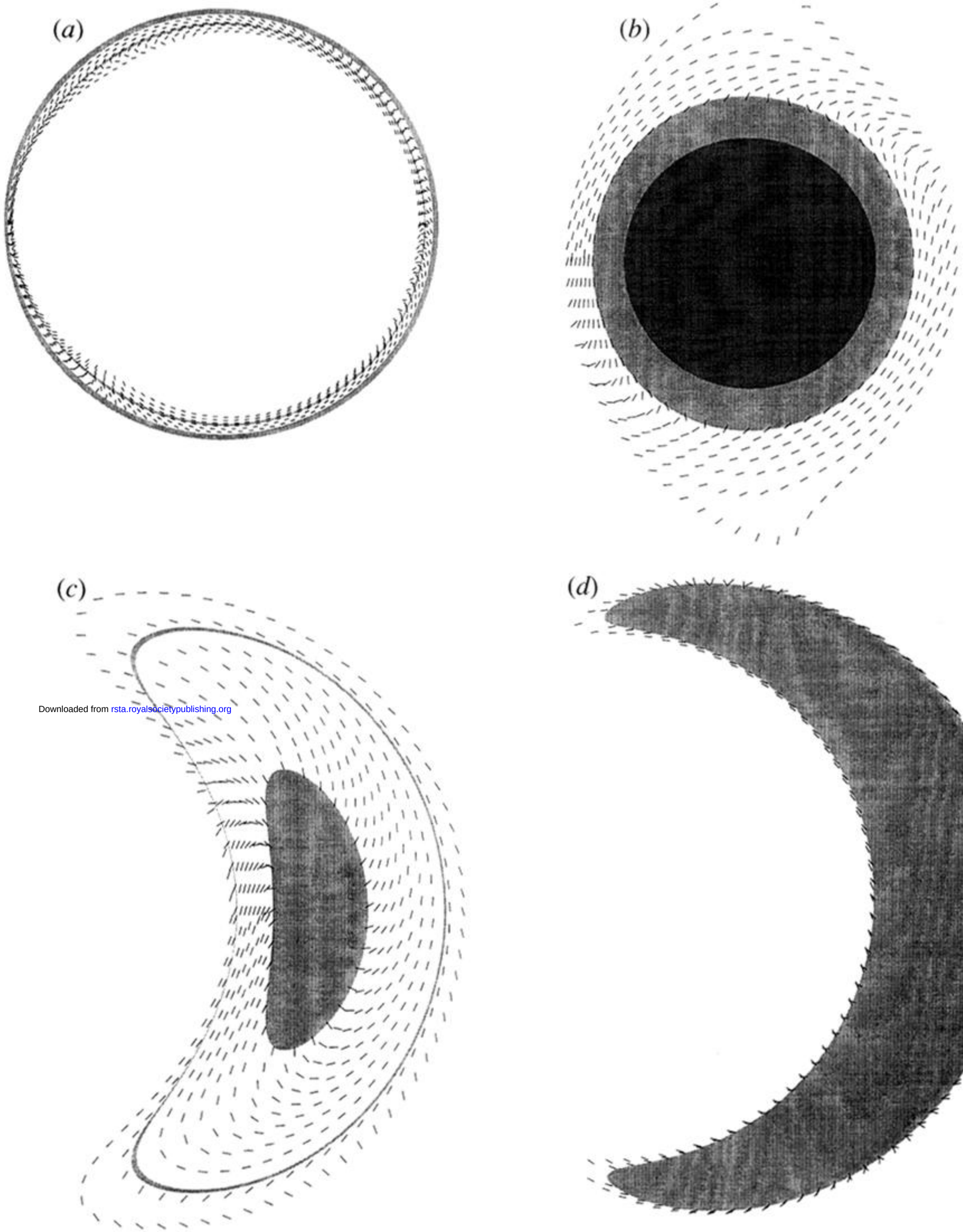

PHILOSOPHICAL TRANSACTIONS OF THE ROYAL SOCIETY A MATHEMATICAL, PHYSICAL & ENGINEERING SCIENCES

igure 6. (*a*) Detail of the four nested zones in cell A. Proceeding from the outside inward, the zones re quasi-periodic, patterned (+3 flips), quasi-periodic, and patterned (+4 flips). (*b*) Detail of the wo nested zones in cell B. Proceeding from the outside inward, the zones are patterned (0 flips), nd quasi-periodic. The dark circle is the inner cylinder. (*c*) Detail of the four nested zones in cell '. Proceeding from the outside inward, the zones are patterned (−1 flips), quasi-periodic, atterned (−2 flips), and quasi-periodic. (*d*) Detail of the two nested zones in cell D. Proceeding rom the outside inward, the zones are patterned (+3 flips), and quasi-periodic.

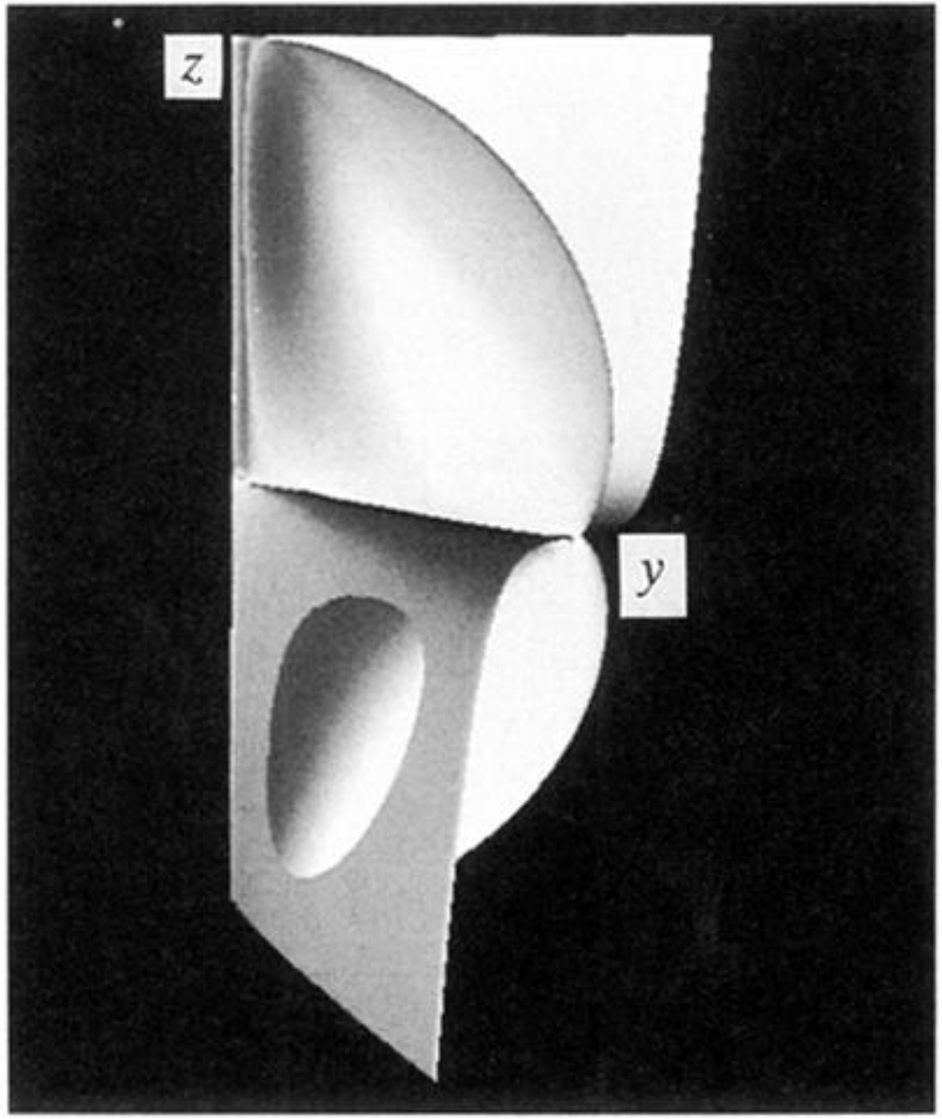

Figure 11. Intersection of the level sets of the Casimir functions C and D with $c = 0.01$ and $d = 1$, in the domain $y \geqslant 0$. The surface associated with C is the warped sheet, and the surface associated with D is the closed bean-shaped surface. The recirculating particle paths in this flow follow the intersections of the level sets of C and D.

PHILOSOPHICAL TRANSACTIONS OF THE ROYAL SOCIETY A MATHEMATICAL, PHYSICAL & ENGINEERING SCIENCES